Journal of Experimental Botany, Vol. 60, No. 2, pp. 461–486, 2009
doi:10.1093/jxb/ern341

Journal of Experimental Botany
www.jxb.oxfordjournals.org

DARWIN REVIEW

The power and control of gravitropic movements in plants: a biomechanical and systems biology view

Bruno Moulia[1,2,*] and Meriem Fournier[3]

[1] INRA, UMR 547 PIAF, F-63100 Clermont-Fd Cedex 01, France
[2] Université Blaise Pascal, UMR 547 PIAF, F-63177 Aubiere Cedex, France
[3] AgroParisTech, UMR 1092 LERFOB, ENGREF, 14 Avenue Girardet-CS 4216, F-54000 Nancy Cedex, France

Received 30 September 2008; Revised 29 November 2008; Accepted 2 December 2008

Abstract

The study of gravitropic movements in plants has enjoyed a long history of research going back to the pioneering works of the 19th century and the famous book entitled '*The power of movement in plants*' by Charles and Francis Darwin. Over the last few decades, the emphasis has shifted towards the cellular and molecular biology of gravisensing and the onset of auxin gradients across the organs. However, our understanding of plant movement cannot be completed before quantifying spatio-temporal changes in curvature and how they are produced through the motor process of active bending and controlled by gravisensing. This review sets out to show how combining approaches borrowed from continuum mechanics (kinematic imaging, structural modelling) with approaches from physiology and modern molecular biology has made it possible to generate integrative biomechanical models of the processes involved in gravitropism at several levels. The physiological and biomechanical bases are reviewed and two of the most complete integrative models of the gravireaction organ available are then compared, highlighting how the comparison between movements driven by differential growth and movements driven by reaction wood formation in woody organs has provided highly informative key insights. The advantages of these models as tools for analysing genetic control through quantitative process-based phenotyping as well as for identifying target traits for ecological studies are discussed. It is argued that such models are tools for a systems biology approach to gravitropic movement that has the potential to resolve at least some of the research questions raised 150 years ago.

Key words: Architectural modelling, biomechanics, functional ecology, gravisensing, gravitropism, growth kinematics, mechanoperception, phenotyping, reaction wood, systems biology.

Introduction

Gravitropism is a highly salient trait of land plants and a primary requisite for plant life on Earth. It is found in all land-based plant species, and at every stage, from the delicate coleoptiles, hypocotyls, and roots of seedlings through to the robust stem of adult maize plants and even in the huge trunks of the largest trees (Moulia *et al.*, 2006). It therefore comes as no surprise that there has been a continuous research effort dedicated to gravitropism from the outset of plant physiology and plant biomechanics in the late 19th century (Darwin and Darwin, 1880; Sachs, 1882) right through to the most advanced spatial research of the 21st century. In 1880, Charles Darwin and his botany-trained third son Francis published '*The power of movement in plants*'. The book had a profound influence on botany, pioneering in-depth kinematic studies of plant movement and partly paving the way for the later discovery of auxin, a major plant hormone involved in tropisms, yet the title was equally evocative, and has been retained by many reviews and textbooks (Salisbury and Ross, 1992). The current revival of auxin transport, driven by genetics and developmental biology with the added boost given by space research agency studies into how gravity affects

* To whom correspondence should be addressed. E-mail: moulia@clermont.inra.fr
Abbreviations: α_T, tip angle; γ, inclination angle; κ, curvature; s, curvilinear abscissa; t, time; P, turgor pressure; V, cell volume; Π, osmotic opressure; ε, longitudinal stain; σ, longitudinal stress; t_s, stimulation time; τ_r, reaction time; IAA, indole acetic acid.

plants, has produced a wide range of excellent reviews on the recent biological studies into gravitropism (Firn and Digby, 1980; Hejnowicz, 1997; Kiss, 2000; Kutschera, 2001; Blancaflor and Masson, 2003; Haswell, 2003; Perbal and Driss-Ecole, 2003; Morita and Tasaka, 2004; Iino, 2006; and the recent book '*Plant tropisms*' edited by Gilroy and Masson, 2008). The central focus of this Darwin series review is not to add another update on the very latest published research on the genetics or functional genomics of graviperception, but rather to pick up the thread of the Darwins' pioneering work, by showing how the tools and concepts from physics and mechanical engineering can complement standard physiological and modern genetic–molecular approaches to unravel some of the mysteries behind the power and control of gravitropic movements.

We start by outlining how gravitropic movement can be quantified using kinematics tools, and then move on to recent developments in bio-imaging borrowed from continuum mechanics. Then dose–response relationships and their relevance to the study of gravity sensors and gravitropism control will be revisited. A third section will be dedicated to the motors underpinning the active bending involved in tropisms and the way physics helps to understand the power involved in movements. We will then be in a position to analyse and compare the major features of two integrative mathematical structure–process models of shoot gravitropism and to discuss the insights offered in terms of systems biology and the architectural modelling of gravitropism. Finally, given that one of the major motivations prompting Charles Darwin to study the power of movement in plants was to find evidence for natural variations and cues to natural selection, we will discuss how far gravitropism underpins a global biomechanical strategy for standing plants (Moulia *et al.*, 2006) and present recent insight on gravitropism in plant ecology (Fournier *et al.*, 2006). Most of our examples will deal with shoot gravitropism, including primary growing organs (e.g coleoptiles, hypocotyles, stems) as well as organs undergoing secondary growth (conifer and dicot stems), but most of the notions and tools presented can be transposed to roots, and, with some technical extension (Silk, 1984; Coen *et al.*, 2004) to organs undergoing surface expansion (e.g. leaves).

Lastly, as this review is designed for a general biologist audience, there is no need for an advanced background in mechanics or maths. For the crucial points at least, we have tried to stick to the pedagogical 'Rule of Four', which states that topics should be presented at the same time (i) verbally, (ii) geometrically or diagrammatically through sketches, (iii) algebraically with equations whenever possible, and (iv) numerically, with orders of magnitude (Hughes-Hallet *et al.*, 1996).

The kinematics of curvature in growing organs: beyond the so-called curvature angle

From 'curvature angle' to spatio-temporal curvature field

The major experimental novelty forming the foundation of Charles and Francis Darwin's work on '*The power of movement in plants*' (1880) was actually a clever, although biased, way to track the movement of organs tips in 3D through optical biplanar projections and manual recording. Kinematics, or the study of changes in position over time, has remained pivotal to (i) establishing quantitative phenomenological descriptions of the active movements of plants, and (ii) to quantifying possible relationships with candidate mechanistic models.

Through their kinematic description, the Darwins first noted that, although most plants display a spontaneous 3D helicoidal movement during growth called circumnutation, during gravitropic reactions the horizontal component of the movement was reduced to a very low level so that the plant axis bent mostly within a vertical plane (Darwin and Darwin, 1880), a plane in fact defined by the gravity vector *g* and the axis of the organ (Correll and Kiss, 2008). Figure 1 shows three examples of this kind of gravitropic movement within the vertical plane in three species. As noted by the

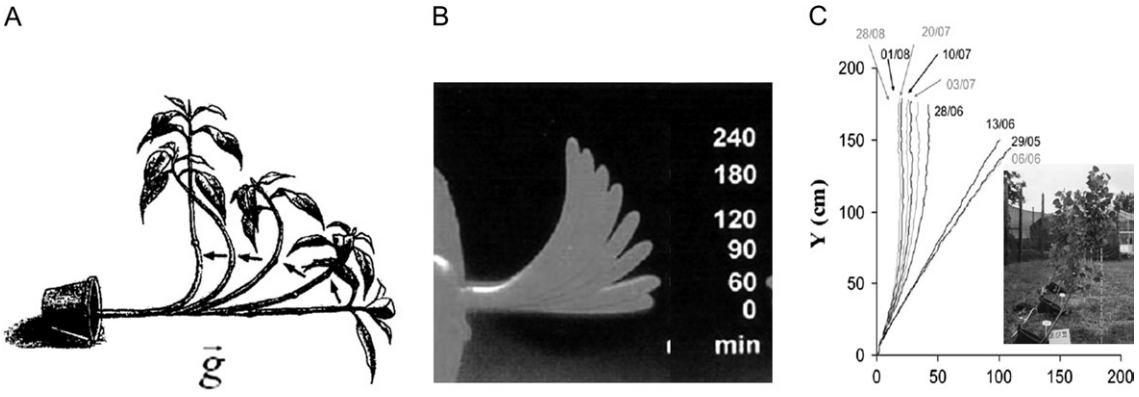

Fig. 1. Negative gravitropic movements in (A) *Impatiens glandulifera* stems (taken from Kutschera, 2001, reprinted from *Advances in Space Research* © 2001 with kind permission from Elsevier), (B) wheat coleoptile (taken from Philippar *et al.*, 1999, © National Academy of Sciences, USA), (C) a poplar tree (*Populus deltoides*×*nigra*) (taken from Coutand *et al.*, 2007, www.plantphys.org, © American Society of Plant Biologists). Note that (A) reproduces drawings from one of the oldest movies of gravitropic movement, made by Pfeffer in 1904. A video transcription is available at http://www.dailymotion.com/video/x1hp9q_wilhem-pfeffer-plant-movement_shortfilms.

Darwins, the tropic movement involves spatio-temporal changes in the local stem form. A 3 cm long coleoptile from a grass seedling, a 50 cm dicot stem or a young 2 m high tree all share some obvious similarities: active tropic bending is distributed along the growing zones of the organs and all the stems tend to curve and de-curve in different places over time to reach a vertical and mostly straight form at the end of the movement. The tip of the organ in Fig. 1A and C even appears to reach a steady vertical orientation whereas the base is still curving. These spatio-temporal changes in the distribution of curving and growth make it difficult to characterize gravitropic movements via any single global measurement at the whole-organ level. This means that a significant issue in the study of tropism is how to relate local changes in angles all along the organ to the global change in its shape during the movement, to understand the role played by growth and the underlying biological control. Despite these observations and the early demonstration by the Darwins that the tip played a much lesser role in shoot gravitropism than in phototropism (Darwin and Darwin, 1880, confirmed by modern studies, Firn *et al.*, 1981; Tasaka *et al.*, 1999), tropism research has persisted with a long tradition of only measuring the inclination angle of the tip α_T. To account for the fact that the tip of the stem might not be exactly perpendicular to the pot but display an initial inclination angle $\alpha_{T(0)}$ due to imperfect straightness and passive mechanical bending under self-weight, some investigators have defined a 'curvature angle' as the change in tip inclination angle over time, i.e. the difference $\Delta\alpha_{T(t-t0)}=\alpha_{T(t)}-\alpha_{T(t=0)}$ (Hoshino *et al.*, 2007; Tanimoto *et al.*, 2008, to cite only recent papers). The terminology used is itself quite varied, ranging from the frequent 'curvature angle' or 'bending angle' to the more confusing 'curvature (degrees)' (the reason why it is so confusing will become clear later), but much more problematically, the spatial positioning of this angle along the organ is not standardized. Figure 2 displays two examples of drawings defining the curvature angle taken from the literature: Fig. 2A clearly defines a mean angle for the overall organ after a significant straightening, whereas Fig. 2B defines the tangent angle at the tip while carefully avoiding the highly tapered zone at the tip where small errors in locations can induce significant errors in the measurement of the angle, and Fig. 2C sits somewhere in the middle. Although the angles measured on an organ according to Fig. 2A and B may change in the same direction over gravitropic movement, there is by no means a biunivocal relation between the two angles, as shown in Fig. 3 (Coutand *et al.*, 2007). Indeed, different angular distributions along the organ can lead to similar tip angles even at the same organ length (Fig. 3A–D)! Moreover, it is equally confusing to compare the changes in 'curvature angles' of two organs of different lengths (Silk, 1984; Iino *et al.*, 1996), since a similar rate of change in angle with position along the organ (per unit length) would yield different tip angles (Fig. 3 E)! All this might be quite confusing when attempting to analyse the kinetics of angle changes during tropism.

This problem of the relation between local angle changes and total tip angle has long since been tackled in differential geometry, calculus, and mechanics by defining the local rate of change in angle with position along a line per unit length (Fig. 3F), a quantity consistently used worldwide under the term 'curvature' (Edwards and Penney, 1994). Stated in another way, if s is the distance along the curved line joining the centres of the successive cross-sections (the curvilinear abscissa) and $\alpha_{(s)}$ is the local inclination angle of the tangent at s, then the curvature at this point $\kappa_{(s)}$ is

$$\kappa_{(s)} = \frac{d\alpha_{(s)}}{ds} \quad (1)$$

where $d\alpha_{(s)}$ is expressed in radian and is thus a dimensionless quantity (see Fig. 3F), and ds is a length. Therefore, $\kappa_{(s)}$ is a unit of length^{-1} and thus the SI unit of m^{-1}, but its most usual units in plant kinematics are cm^{-1} or mm^{-1}. This quantity has long been used in plant biomechanics (Moulia *et al.*, 1994), and although introduced to the world of plant physiology some time ago (see the landmark reviews by Silk and Erickson, 1978; Silk, 1984; Cosgrove, 1990*a*, for pioneering studies in tropism), it has only recently made significant headway for calculating plant tropisms (Meskauskas and Moore, 1998; Basu *et al.*, 2007; Coutand *et al.*, 2007; Chavarrìa-Krauser *et al.*, 2008; among others).

Both curvature field $\kappa_{(s)}$ at a given time t and the field of inclination angle $\alpha_{(s)}$ can be measured via several techniques: (i) photographs, 2D digitizing and curve fitting (Moulia *et al.*, 1994; Meskauskas and Moore, 1998); (ii) 2D video, image analysis, and curve fitting (Basu *et al.*, 2007; Chavarrìa-Krauser *et al.*, 2008); and (iii) 3D magnetic digitizing and curve fitting (Coutand *et al.*, 2007). It should be noted that local fits (e.g. local polynomials or splines) are to be preferred over global polynomial fits as they display less bias (Moulia *et al.*, 1994; Coutand *et al.*, 2007).

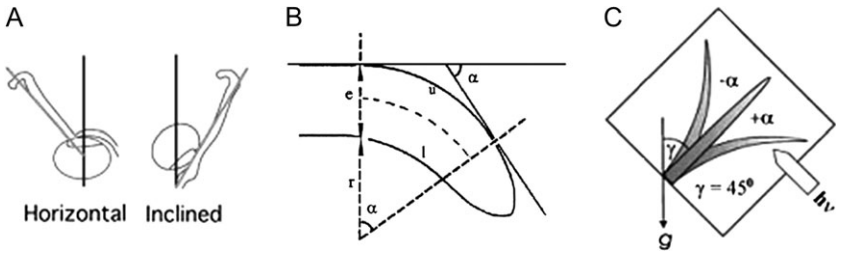

Fig. 2. Examples of the various definitions of 'curvature angle' (A) Hoshino *et al.*, 2007, reproduced by kind permission of the Botanical Society of Japan, (B) Perbal *et al.*, 2002, © *Physiologia Plantarum*, (C) Galland, 2002, and reproduced by kind permission from Springer. Note that the angle has been measured with reference to the vertical, the horizontal or even the initial position of the tilted stem.

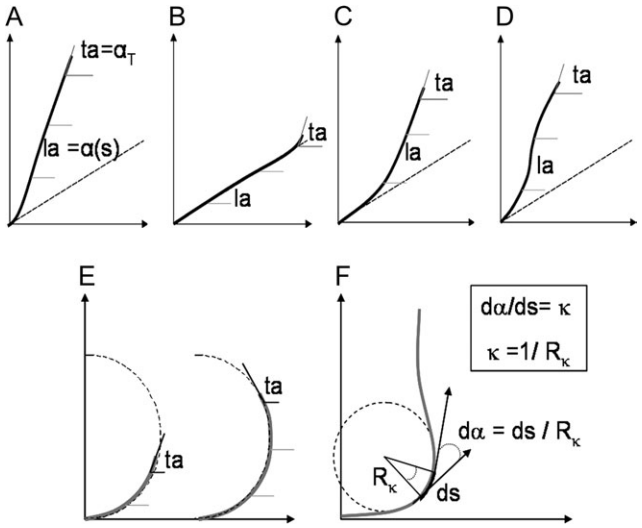

Fig. 3. Relations between tip angle (ta), local angles (la), and curvature distribution: (A, B, C, D) different distributions of the local angle (la) along the organ displaying the same tip angle $ta=\alpha_T$ (from Coutand *et al.*, 2007, www.plantphys.org, © American Society of Plant Biologists), (E) organs with similar rates of changes in angle with position along the organ sits along a circle, but different lengths yield different tip angles, (F) definition of the curvature as the rate of changes in angle with position along the organ per unit length $\kappa=d\alpha/ds$: the angle $d\alpha$ in radians is equal to the length of the arc of the tangent circle at point s divided by the radius of this circle $R\kappa$ (1 rad is the angle subtended at the centre of a circle by an arc equal in length to the radius of the circle, approximately 57°17). The angle $d\alpha$, in radian is thus dimensionless. The curvature $\kappa=d\alpha/ds$ is the inverse of the radius of curvature and has units of the inverse of a length (e.g. cm^{-1}).

Curvature has many advantages. It is a local quantity that can be measured independently of the reference frames. The relationship between angle $\alpha_{(s)}$ and $\kappa_{(s)}$ reflects the fact that local curving influences the angle of inclination. Indeed, the increment of angle $d\alpha_{(s)}$ between s and $s+ds$ is $d\alpha_{(s)}=\kappa_{(s)}ds$, and thus the change in angle $\Delta\alpha$ between the base $s=0$ and the tip $s=L$ is simply the sum of all the successive $d\alpha$ between the two positions (Fig. 3F), i.e.

$$\Delta\alpha_{(\text{base}\rightarrow\text{tip})} = \alpha_{T(s=L)} - \alpha_{B(s=0)} = \sum_{s=0}^{s=L} d\alpha_{(s)} = \int_{s=0}^{s=L} d\alpha_{(s)} = \int_{s=0}^{L} \kappa_{(s)} ds \qquad (2)$$

where L is the length of the organ, which can be numerically computed very easily, even with a standard spreadsheet.

Note that equation (2) gives a quantitative explanation of why a longer organ with similar $\kappa_{(s)}$ will display an increased tip angle whereas the actual bending rate is just the same, as noted previously (Fig. 3E; Iino *et al.*, 1996). Indeed, solving equation (2) for a constant curvature κ along the axis yields $\alpha_{T(s=L)} = \alpha_{B(s=0)} + \kappa L$ (equation 2b), which means that the tip angle increases proportionally to the length L of the organ for the same curvature. Numerically, an almost complete gravitropic movement from an initially horizontal and straight position can be represented by a final tip angle $(\alpha_{T(s=L)} - \alpha_{B(s=0)})$ of 1.5 radians (86°). From equation 2b, the mean curvature then comes as $\kappa=1.5/L$ yielding, respectively, curvatures of 0.5 cm^{-1}, 0.1 cm^{-1}, 0.02 cm^{-1} for organ lengths of 3 cm, 15 cm, and 75 cm.

Last but not least, working with the assumption that between-cell adhesion at the middle lamina is maintained [a validated fact, except for certain extreme cell adhesion mutants, as reported in Krupkova *et al.* (2007)] and that there is therefore negligible shear, it is possible to find very simple relationships between curvature changes, diameter, and differential elongation or shrinkage of the upper and lower cell layers. In organs growing only radially through secondary growth, the computation is direct if, in addition to curvature field over time $\kappa(s,t)$, the cross-sectional radius $R(s,t)$ is also known (Coutand *et al.*, 2007). However, to compute elongating organs requires a deeper specification of the growth kinematics (Silk and Erickson, 1978; Silk, 1984; Basu *et al.*, 2007; Chavarrìa-Krauser *et al.*, 2008).

Kinematics of growth and differential growth: unravelling the influences of cell activity and location on curvature changes

As the gravitropic response involves growth, a standard problem in gravitropic studies is to assess how far the effect on the gravitropic phenotypic performance of say a mutation or a change in environment can be ascribed (i) to effects on growth and its spatial distribution along the organ affecting the gravitropic movement, as opposed to (ii) direct effects on the gravisensing pathway (Tanimoto *et al.*, 2008).

Just as for the rate of curvature, elongation growth is also distributed spatially, and this distribution is usually non-homogeneous. As curvature in the primary growing zone involves local differential elongation growth (Tomos *et al.*, 1989), it is not sufficient only to measure the total elongation rate of the organ $v_T = \frac{dL}{dt}$ (v_T is the tip velocity, usual unit=mm h^{-1}, L is the organ length, usual unit=mm) or the (mean) relative elongation rate $RER = \frac{dL}{Ldt}$ (usual unit=h^{-1}). The rationale here is exactly the same as previously used for the comparison between tip angle α_T and curvature field $\kappa(s)$. Cell elongation in organs tends to stretch the cell irreversibly, so that its length increases over time. The intensity of this growth-induced stretch at every position s along the organ can be measured by the longitudinal strain $\varepsilon_{(s,t)}$, i.e. by the change in length dl of a segment of the organ relative to its length l $\varepsilon_{(s,t)} = dl/l$. As this growth-induced stretching is time-dependent, it is usually better specified by the time-rate of changes in strain, $\dot{\epsilon}_{(s,t)} = \frac{\partial \varepsilon_{(s,t)}}{\partial t}$ (δ is the partial derivative, here with respect to time). Thus, the strain rate field specifies at each position the time-rate of changes in the relative distance between two successive cross-sections of the growing organ (Fig. 4A). Some authors prefer to call growth-induced strain rate the Relative Elemental Growth Rate, REGR (Silk, 1984), but 'strain rate' is consistent with standard use in mechanics and is therefore to be preferred.

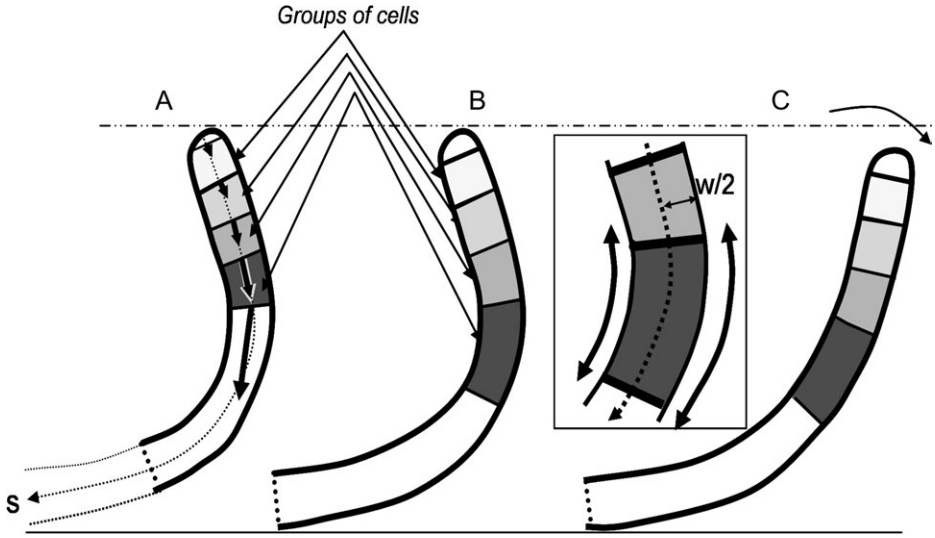

Fig. 4. Kinematics of changes in curvature in expanding organs. Three successive states of the same organ are depicted, with their tips aligned for easier visualization of growth. (A) Initial time t_0: transverse marks are set up at distances s_0,i (i=1–5) from the apex, to follow groups of cells. Dark arrows represents the growth-induced velocity of convective displacement from the apex. Due to differences in growth-induced velocities, marks closer to the tip convect more slowly than marks further away. This is important for the localization of groups of cells over time (see B and C). (B) Example of curvature changes mainly due to convection after a time interval dt: although the spatial distribution of curvature $\kappa_{(s,t)}$ is constant over time, the dark grey segment has moved to a zone of higher curvature by convection and has thus curved accordingly. (C) Example of curvature changes mainly due local changes: as a rapid local change in curvature has occurred between (B) and (C) the dark grey segment has changed its curvature while its longitudinal displacement is negligible. Inset: magnification of the comparison between (A) and (B): the concave side has extended less than the convex side. Comparison between (A) and (C) shows the superposition of convective (A–B) and local (B–C) changes in curvatures over time.

As elongating cells stretch, they also push the downstream cells next in line, with the result that each cell is pushed to move by the preceding cells (Fig. 4A). The more cells that are growing upstream, the larger the push, and the faster the movement velocity (called convection, from the Latin for 'moving with'). Elongation growth thus can be specified using two quantities: (i) the longitudinal velocity field $v_{(s,t)}$, which defines the growth-induced convective velocity of any cross-section in an organ at position s and time t (Fig. 4A), and (ii) the growth-induced strain-rate field $\dot{\varepsilon}_{(s,t)}$. Both are related. The difference in velocity between two successive cross-sections separated by the initial distance ds (Fig. 4A) produces a change in length over time whose relative time-rate is the longitudinal strain rate, i.e.

$$\dot{\epsilon}_{(s,t)} = \frac{\partial v(s,t)}{\partial s}.$$

Finally, as the growth zone in plant organs is mostly subapical, the natural reference frame for the spatial specification of growth-induced fields is taken at the apex (Fig. 4), so that s means distance from the apex (curvilinear abscissa).

Elongation growth has major repercussions for the assessment of curvature changes in elongating organs. Indeed, any given small segment (a group of cells) in the growth zone will, over time, move away from the tip (Fig. 4B), in a similar way to river flow (Silk, 1984). Because of this movement, time-derivatives relative to a given position (distance s measured from the apex) or to a given material segment (group of cells) do not match anymore. But the biological mechanisms involved in perception and motor activity producing curvature changes resides in cells. Consequently, the biologically relevant rate of change of curvature during growth is that of a material segment (group of cells). This is called the material derivative of the curvature, which, to distinguish it from the local derivative in equation (2), is conventionally written $\frac{D\kappa_{(s,t)}}{Dt}$ (the uppercase D distinguishing it from the lowercase d of local derivative and the ∂ of the partial derivative). The point here is that this quantity cannot be estimated simply from the change in curvature at a given position as in equation (2). For example, if an elongating organ displays a steady spatial gradient in curvature, then the local change in curvature is zero (Fig. 4A, B). However, as seen above, there is a growth-induced convective movement along the organ, which means the segment is, in fact, producing a change in curvature, the rate of which depends on (i) how steep the gradient in local curvature is, i.e. on the rate of change of the curvature with position at time t $\frac{\partial\kappa_{(s,t)}}{\partial s}$, and (ii) how fast it moves with respect to this gradient, i.e. on its growth-induced convective velocity $v(s)$ (Fig. 4B). In the most general case, gravitropic primary organs may also display changes in local curvature at position s (noted $\frac{\partial\kappa_{(s,t)}}{\partial t}$), as illustrated by the change between Fig. 4B and Fig. 4C. Therefore to compute the 'real' rate of change in curvature of a segment following the growth-push movement, i.e. the material derivative of curvature, both terms have to be summed and thus the material derivative can be calculated as (Silk, 1984; Chavarrìa-Krauser, 2006)

$$\frac{D\kappa_{(s,t)}}{Dt} = \frac{\partial\kappa_{(s,t)}}{\partial t} + v_{(s,t)}\frac{\partial\kappa_{(s,t)}}{\partial s} \qquad (3)$$

local convective

Graphically (Fig. 4) equation (3) means that the changes in the curvature of a material segment of the organ between Fig. 4A and C (the material derivative) corresponds to the superimposition of (i) the changes between Fig. 4A and B (convective changes in the curvature of the segment) and (ii) the changes between Fig. 4B and C (local changes in curvature). As on-board devices continuously tracking the material curvature of the organ segments are not available yet, equation (3) is just a mathematical expression allowing the material derivative to be computed from the measurement of (i) the local curvature along the organ at various times (i.e. $\kappa_{(s,t)}$) and (ii) growth velocity $v_{(s,t)}$ (to be detailed later). It is also useful to get insights about the positional versus segment-autonomous controls of curvature changes (Chavarria-Krauser, 2006, 2008). Numerically, Silk and coworkers reported, in hooked lettuce hypocotyls, that hook maintenance involved convective successive curving and decurving of stem segments reaching rates up to 2.5 mm^{-1} h^{-1} with no local changes (Silk and Erickson, 1978), whereas dramatic changes in the balance between the two terms were achieved during tropic responses (Silk, 1984). Finally, in organ parts with no longitudinal elongation and thus negligible growth-induced velocity $v_{(s)}$, as in gravitropic stems undergoing radial secondary growth (Coutand *et al.*, 2007) the convective term is always negligible.

The material derivative of curvature $\frac{D\kappa_{(s,t)}}{Dt}$ characterizes the tropic bending response of a small segment of a growing organ. This is the correct quantity to be compared with cellular changes in the same segment, such as a radial gradient in auxin content, differences in cytoskeleton dynamics or differences in levels of gene expression. It is also the proper output of a mechanistic model of the biomechanical motor activity powering the movement (as will be seen in the third section). In such cases, equations (3) and (2) will also be required to reconstruct the changes in stem geometry (length, curvature, and angular distribution, including tip angle) over time from the material rates of curvature changes predicted by the biomechanical model.

Many studies dealing with differential growth have focused on the difference in relative elongation rate between the epidermis on both sides of a curving segment at position s and time t (Myers *et al.*, 1995; Mullen *et al.*, 1998). Indeed, as shown in Fig. 4 inset, curving is related to a higher strain rate in the convex side than in the concave side, with the mean strain rate of the segment sitting between the two. The material rate of curvature changes provides a very straightforward way to compute these differences in growth-induced strain rate in the segment at position s at time t. Indeed, if w is the width of the organ in the (local) plane of bending, so that the epidermis on the convex side sits at $(s,+w/2)$ and the epidermis of the concave side sits at $(s,-w/2)$, then the differences in growth-induced strain rate between the convex and the concave sides can be readily estimated from the material derivative as:

$$\dot{\epsilon}_{(s,t,+w/2)} - \dot{\epsilon}_{(s,t,-w/2)} = \frac{D\left(\kappa_{(s,t)}w\right)}{Dt} = \frac{\partial\left(\kappa_{(s,t)}w\right)}{\partial t} + v_{(s,t)} \cdot \frac{\partial\left(\kappa_{(s,t)}w\right)}{\partial s} \qquad (4)$$

If the width w changes slowly with time and position (low tapering), as tends to be the case in growing stems and roots (equation 4), the derivatives of w can be neglected when applying the Chain Rule in calculating the partial derivatives of the $\kappa.w$ products in equation (4) then yields:

$$\dot{\epsilon}_{(s,t,-w/2)} - \dot{\epsilon}_{(s,t,+w/2)} \approx \frac{D\kappa_{(s,t)}}{Dt} \cdot w \qquad (5)$$

Equation (5) states that differential growth is approximately proportional to the material rate of curvature changes multiplied by the organ width, so that wider organs require more differential growth to achieve the same material rate of curvature changes and thus the same tropic movement. For example, an observed material rate of curvature changes of 0.1 mm^{-1} h^{-1}on an organ width of 0.5 mm would correspond to a difference in growth-induced strain rates of 5% h^{-1}, whereas this difference would come to 10% h^{-1} if the organ width is 1 mm (see Silk, 1984, for a more complete presentation including large strain rates that should be considered in cases where the product $\kappa.w > 0.3$).

Direct characterization of growth-induced strain rates in the epidermis is a possible option (Mullen *et al.*, 1998), but the results may be less accurate and equation (5) would still be required in order to relate differential growth to the induced tropic curvature. Equation (5) conveys the important kinematical fact that the effect of differential growth on gravitropic bending [and thus on curvature angles through equation (2)] depends on the width of the organ. It will be shown later that the dependence on size of the material changes in curvature is even stronger when taking into consideration the biomechanical motor and the resisting processes involved in producing the active bending movement (see third section).

Last but not least, the rationale for considering the material derivative also applies to any content variable along the organ (Silk, 1984), such as, for example, the concentration in auxin or any other substance (pH, calcium, pectins, etc). Indeed, when there is a gradient in concentration along the organ (a most common feature), then the local rate of change alone is not enough, as convective changes also have to be considered such as in equation (3). Since concentration is based on volume and volume also changes over time, a dilution term has to be added. This is called the continuity equation, and can be found in most papers analysing growth mechanisms (as summarized in Basu *et al.*, 2007), and a pedagogical version can be found in Silk (1984).

Several methods based on time-lapse photography or video could be used to measure the growth-induced strain rate field $\dot{\epsilon}_{(s,t)}$ and velocity field $v_{(s,t)}$ and combine them with the curvature field $\kappa_{(s)}$ to calculate the material derivative of

curvature (or any material rate of change of substances). Note that to estimate properly the time-derivatives in equation (4), the time lapse needs to be small enough to yield a mean growth-induced strain between two successive frames that is smaller than 0.2 (Silk, 1984). This condition is not always fulfilled in published data; overlong time lapses feature not just in all the original articles (Sachs, 1882) but in some of the more recent studies as well (Fukaki *et al.*, 1996).

The traditional method has been to perform marking experiments as depicted in Fig. 4 and to record their position over time with time-lapse photography using a appropriate time lapse (e.g. on stem growth; see Girousse *et al.*, 2005). Genetic mosaics have been elegantly used to build in marks (Coen *et al.*, 2004), but their use for kinematics requires a step-by-step analysis decrementing the past history. Surprisingly, despite the initial use by Sachs, few gravitropic studies have used marking experiments with small time lapses (Selker and Sievers, 1987; Mullen *et al.*, 1998; Miyamoto *et al.*, 2005). In contrast with the studies on growth responses where kinematics has became a standard (as rightly pointed out by Basu *et al.*, 2007), most gravitropism studies persist with the so-called 'curvature angle' to characterize the phenotypic gravitropic response. This might be partly related to the fact that marking experiments are seen as somewhat tedious and old-fashioned. More recently, bio-imaging techniques have been developed based on time-lapse photos or videos and automatic structure–tensor (Schmundt *et al.*, 1998) or image-correlation analysis (van der Weele *et al.*, 2003; Suppato *et al.*, 2005). These techniques have been successfully applied to geotropic roots (Basu *et al.*, 2007; Chavarrìa-Krauser *et al.*, 2008). A user-friendly freeware is already available, yet too restrictively named KineRoot as it can actually be used for kinematical analysis of any gravitropic response (Basu *et al.*, 2007). These tools are likely to increase and improve in the near future, and there is hope that these versatile tools will soon be instrumental in making kinematical bio-imaging a viable approach for the majority of teams studying gravitropic responses.

New insights from curvature kinematics: two examples

The kinematic method has been instrumental in characterizing the Distal Elongation Zone in roots (DEZ) and in defining its specific function for root-based gravitropic curvature (Mullen *et al.*, 1998; Chavarrìa-Krauser *et al.*, 2008). This became possible thanks to the kinematic approach, which is able to distinguish between mean strain rate of the segment, (material) changes in curvature and differential strain rates with a high spatio-temporal resolution. More recently, kinematic studies were able to reveal a clear root phenotype for the *pin3-3* mutants in *Arabidopsis* (Chavarrìa-Krauser *et al.*, 2008). PIN3 is a putative efflux-transporter of auxin and a central candidate gene for the control of radial gradient in auxin concentration, but its function had previously been unclear since there had been no way decisively to pinpoint the phenotype of *pin3* mutants (Morita and Tasaka, 2004).

Another example is the characterization of a spatio-temporal pattern of gravitropic curving and autotropic decurving that seems to be generic to many plants ranging from trees to small primary organs, despite largely different sizes (Moulia *et al.*, 2006; Coutand *et al.*, 2007). As shown by the plot of the spatio-temporal curvature field in Fig. 5, the initial phase of spatially homogeneous up-curving destabilizes into a counter-curving spreading downward. This counter-curving occurs before the tip has overshot the vertical (Fig. 1C). It is therefore not due to a graviperception of the inclination angle and has thus been called autotropic ((Firn and Digby, 1979; Tarui and Iino, 1997; but see also Stankovic and Volkmann, 1998). Similar curving dynamics have been reported for wheat and oat coleoptiles (Fig. 1B) and in the stipe of the Coprinus fungi (Meskauskas and Moore, 1998; Meskauskas *et al.*, 1999*a*; Moulia *et al.*, 2006). However, this very efficient movement, allowing rapid stabilization of the tip at a vertical position through autotropic control, is not found in all the plants (Sierra *et al.*, 2008; Fig. 1A). Autotropism will be discussed in more detail in the modelling and ecology sections.

These two examples demonstrate that a spatio-temporal kinematics approach, based on the distribution of the material time-derivative of the curvature and the distribution of growth-induced strain rates and velocities, has led to a deeper understanding of the mechanisms involved in gravitropism, increased the capabilities of phenotyping mutants, and opened the search for common patterns of regulation in different organs and/or species.

Dose–response curves for angular perception, gravitropic sensitivity and control

Macroscopic phenomenology: the sine rule

Once the movement has been properly quantified, the next step may be to establish a dose–response curve relating the kinematics

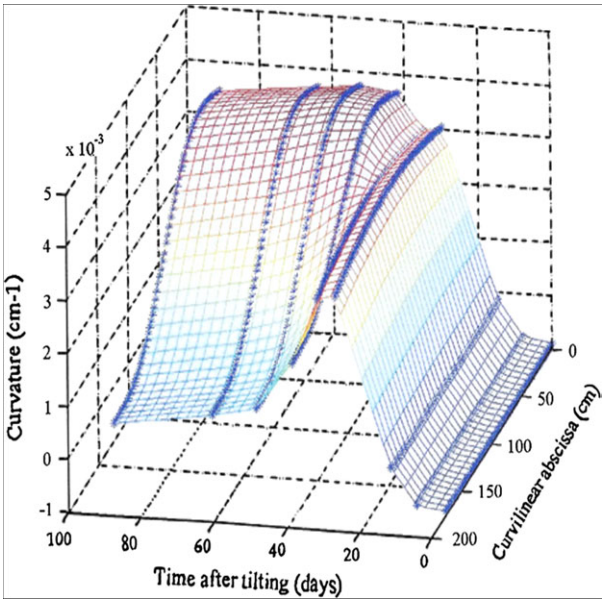

Fig. 5. Spatio-temporal field of curvature during the gravitropic-autotropic straightening movement of poplar stems (Coutand *et al.*, 2007, www.plantphys.org, © American Society of Plant Biologists).

of bending to gravitational stimuli. This approach started with Sachs (1882) defining the 'sine law', but it remains an important issue, taking advantage of microgravity spatial and Earth-based experiments (Galland, 2002; reviewed in Perbal *et al.*, 2002; Correll and Kiss, 2008). Indeed, such quantitative dose–response relations are an important tool in assessing possible cellular and molecular models to explain gravisensing (e.g. is starch-statolith movement fast enough to fit with the dose–response curves?). Moreover, they provide the foundations for building more integrative models of the gravitropic response.

A dose–response curve is a quantitative relation f between gravitropic response and the variables triggering the stimulation. As several responses can be studied (changes in tip angle, changes in curvature, molecular events involved in the graviperception pathway, among others), but do not need to be specified at this point, the response is noted as Ω_g. The stimulation can be local, may involve gravity $\vec{g}$ (or any acceleration), stimulation angle [usually noted γ (Fig. 1C)], and stimulation time t_s, i.e. the duration during which the gravisensors have been submitted to the stimulus (and probably other variables as seen previously). Hence, the dose–response curve is, at least, an equation of the form:

$$\Omega_g = f(g, \gamma_{(s,t)}, t_s, \ \ldots) \tag{6}$$

As different organs display different gravitropic directions (some stems are orthogravitropic, growing vertically, while others, like many branches, are plagiogravitropic and grow laterally), a Gravitropic Set-point Angle (GSA) γ_{GSA} has been defined (Digby and Firn, 1995) and so the relevant stimulus was held to be the difference between the absolute stimulation angle γ and the GSA (but see Meskauskas *et al.*, 1999*a*, *b*). Then equation (6) becomes:

$$\Omega_g = f(g, (\gamma_{(s,t)} - \gamma_{GSA(s,t)}), t_s, \ \ldots) \tag{6b}$$

From what we have seen previously, it is tempting to consider gravitropic responses in terms of the material derivative of the curvature. Up to now, however, direct studies of dose–response curves were performed on the basis of the tip angle α_T, so that Ω_g was characterized as the change in tip inclination angle over time $\Delta\alpha_T(t)=\alpha_T(t)-\alpha_T\ (t=0)$ (Fig. 2C).

Iino *et al.* (1996) made an important step towards studying the response to stimulation angle (at constant gravity). They studied maize and rice coleoptiles which tended to grow orthotropically (GSA $\gamma_{GSA}=0$). When tilted to an initial horizontal stimulation angle $\gamma=\pi/2$ radians$=90°$) measured at the tip (Fig. 6A), the changes in tip angle $\Delta\alpha_T(t)$ clearly displayed a typical gravitropic response with S-shaped kinetics. There was a lag in the curvature response (reaction time τ_r) followed by a rapid acceleration phase reaching a maximal rate of changes in $\Delta\alpha_T(t_s)$, after which changes in angle levels plateaued out.

When different experiments with different smaller initial simulation angles were performed, the lag-time remained almost unchanged, but the rate of changes clearly decreased. The response could thus be expressed as a simple relation between the rate of change of the tip angle $d\alpha_T/dt$ and the stimulation angle. However, as Iino *et al.* (1996) rightly pointed out, the stimulation angle changed continuously in such gravitropic experiments as soon as the reaction time τ_r was overreached (and remember that it also changes differently everywhere: Fig. 2)! and then both the stimulation angle and stimulation time would depend on time and position [$\gamma(s,t)$ and $t_s(s,t)$]. However, considering the rate of change of the tip angle just after the end of the reaction time $\frac{d\alpha_T}{dt}(t=\tau_r)$ made it possible to characterize the dose–response to a defined stimulation angle with a stimulation time t_s equal to the reaction time τ_r. Characterizing the rate of change of the tip angle just after the end of the reaction time was not straightforward though, because there exists an acceleration phase just after the onset of the gravitropic bending, whose characteristics may be related to some intrinsic limitations in differential growth acceleration rather than to gravisensing. However, Iino *et al.* (1996) noticed that the almost constant rate of tip angle changes was reached before two reaction times ($t=2\tau_r$), i.e. before the perception of the changing stimulation angle may have been transduced into a new response. This means that the dose–response relationship could be properly defined as the influence of the initial stimulation angle applied during a stimulation time equal to the reaction time ($t_s=\tau_r$) on the steady rate of tip angle changes $d\alpha_T/dt$ measured at a time lower than twice the reaction time ($t<2\tau_r$). This made it possible to establish an elegant relationship to the sine of the initial stimulation angle γ, with a correlation coefficient of $\approx$0.9 (Fig. 6B). This pattern, which has been found repeatedly in several species and organs (Tarui and Iino, 1997; Galland, 2002, in oats), formed the basis of Sachs' 'sine law' (Sachs, 1882) stating that: 'the intensity of the gravitropic change in tip angle for a given stimulation time t_s and a given gravity g is proportional to the sine of the stimulation angle of the plant relative to the direction of the gravitational field vector', i.e. $\frac{\partial\alpha_T}{\partial t}(\tau_r < t < 2\tau_r, g) = k_{SA}\sin(\gamma_0)$, with k_{SA} being a constant with a time^{-1} unit, and the subscript SA coding for 'related to the response to the stimulation angle at constant stimulation time'. This relation can be extended to plants with different GSA. Moreover, as the tip angle can be also defined with respect to the vertical as the current angle $\gamma_T(t)$, a more general formulation for quasi-static variations of the stimulation angle would be:

$$\frac{\partial\gamma_T}{\partial t}(g) = -k_{SA}\sin\left(\gamma_{T(t-\tau_r)} - \gamma_{GSA}\right) \tag{7}$$

where $\gamma_T\ (t-\tau_r)$ is the tip angle one reaction time before present time t. Typical numerical values for this law (equation 7) in maize coleoptile were $\tau_r \approx$30 min and $k_{SA} \approx 0.4°\ \text{min}^{-1} \approx 0.4$ radians h^{-1} (Iino *et al.*, 1996), but considerable natural variations have been reported (see section, 'Back to the HMS Beagle').

This sine law can be interpreted as the active component of the gravity vector $\vec{g}$, being transverse to the longitudinal axis of the axis (Sachs, 1882). Note also that if the γ angles are expressed in radians, then for a rather small $\left(\gamma_{T(t-\tau_r)} - \gamma_{GSA}\right)$ (i.e. less than $\pi/4$ rad$=45°$) the Taylor series of the sine yields:

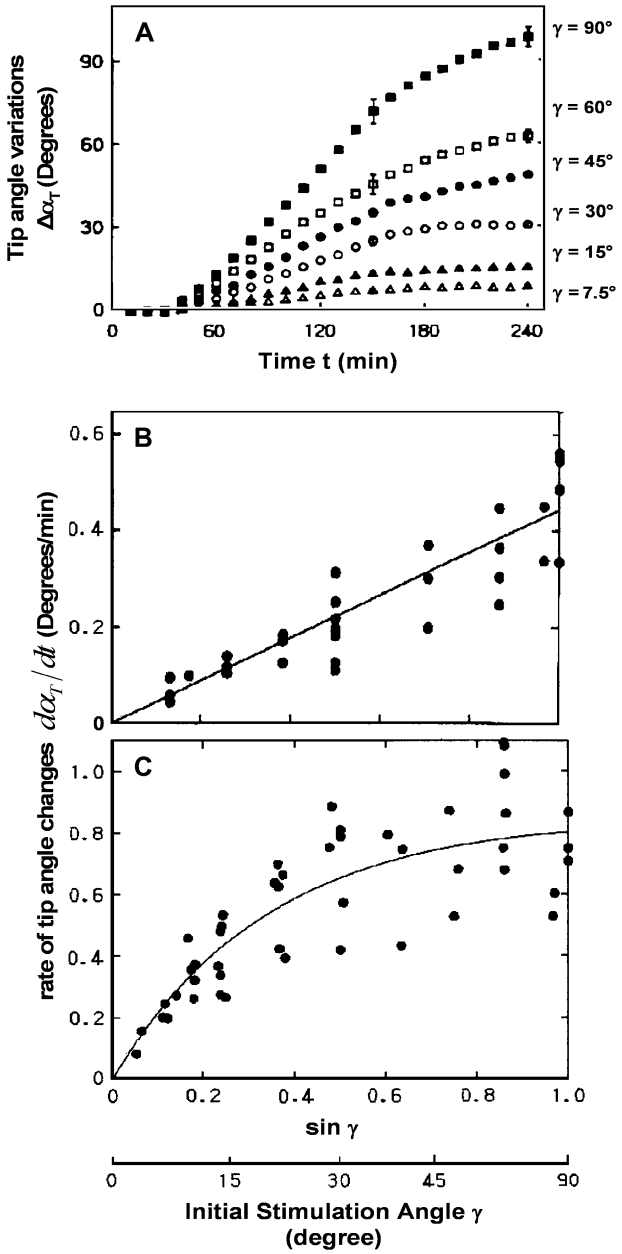

Fig. 6. Dose–response curves for the rate in change in tip angle versus initial stimulation angle γ (from Iino *et al.*, 1996, reproduced by kind permission of Blackwell Publishing). (A) Kinetics of changes in tip angle at different initial stimulation angle γ for maize coleoptiles; (B, C) relation between the rate of change in tip angle and the sine of the stimulation angle in maize (B) and rice (C).

$$\frac{\partial \gamma_T}{\partial t}(g) \approx -k_{SA}\left(\gamma_{T(t-\tau_r)} - \gamma_{GSA}\right) \qquad (7b)$$

with less than 10% approximation.

Defining the dose–reponse as in equation 6B requires the additional analysis of the effects of the stimulation time t_s and of the gravity-induced acceleration g. In tilting experiments run on Earth, as in Iino *et al.* (1996), it is, however, impossible to control stimulation time t_s (as we have seen that this is determined by the reaction time τ_r of the plant), nor the gravity-induced acceleration g. To do so takes two other types of experiments (i) rotating the plants slowly around their axis in a 2D clinostat or randomly in a 3D clinostat, making the gravitational stimulus isotropic (see Larsen, 1969, and Pickard, 1973, for ingenious experiments using a 2D clinostat), or (ii) using a centrifuge and/or microgravity to model the acceleration and mimic the range from hypergravity to microgravity (reviewed in Correll and Kiss, 2008). These options all have their limits, in particular, the fact that fast mechanical deformations (bending during clinostatic rotation, vibrations, etc) might activate mechanosensors that may affect both growth (thigmomorphogenesis; Coutand and Moulia, 2000) and the gravisensitivity itself (LaMotte and Pickard, 2004; Telewski, 2006). These studies mostly confirmed that the sine law gives a good fit for small stimulation times t_s close to the minimal time that yielded a noticeable bending response (called the presentation time τ_p; Larsen, 1969); or at least for stimulation times that are small enough ahead of the reaction time ($t_s/\tau_r < 10^{-1}$).

Considering larger stimulation times or different acceleration fields yielded more complex dose–response curves. The relation between the response and t_s (or the gravistimulatory dose $S_d = g \times t_s$) exhibits a log or, more probably, a hyperbolic shape (Perbal *et al.*, 2002), the latter suggesting that even very small doses (or presentation times) may be sensed and that saturation is to be expected with large stimulations. Moreover, increasing the presentation time yielded an increasingly skewed curve for the response to the stimulation angle γ_T. This curve displayed maximal responses at angles close to $2\pi/3$ rad (120°), thus departing from a sine distribution, especially for angles higher than $\pi/2$ rad (90°) (Larsen, 1969; Galland, 2002). Several models have introduced an inhibitory multiplicative ($1-\cos(\gamma_T)$) term related to the effect of the axial component of gravity (see Audus, 1964, for a review).

Even at small t_s and constant $g \times t_s$, Iino *et al.* (1996) reported a clear saturation for the response to rice coleoptiles (Fig. 6C), showing that the range of validity of the sine law may be species-dependent. Finally, when graviresponses occur with light (Galland, 2002), which is a feature relevant to shoot gravitropism in natural conditions, there was a phototropism-mediated change in GSA (with exponential dependency on fluence rate), yielding photo-gravitropic equilibrium (Galland, 2002: see Iino, 2006, for a more detailed review and discussion).

These more complex effects, in particular, the sine and cosine terms, have been interpreted as revealing underlying competing mechanisms in the cellular–molecular process of graviperception. However, as shown before, the tip-angle response considered in all these studies is an integration of all the local bending responses along the organ [see equation (2)]. Moreover, in stems and coleoptiles the gravisensing competency is distributed in the endodermis that spans the entire stem length (Tasaka *et al.*, 1999; Morita and Tasaka, 2004). The previous dose–responses are thus really big black boxes! Lastly, as soon as stimulation time t_s creeps beyond reaction time τ_r, the stimulation angle $\gamma(s,t)$ changes continuously (and this will affect the response from as early as $t_s > 2\tau_r$).

It would be much more informative to establish dose–response curves directly incorporating the material rate of curvature changes $\frac{D\kappa_{(s,t)}}{Dt}$ and equations (4) and (5), but to the best of our knowledge, this has not yet been done in shoot organs [the situation is a bit different in roots as there is consensus that gravisensing is restricted to the tip: see Chavarrìa-Krauser *et al.* (2008) for a detailed kinematical analysis in root systems, but see also Wolverton *et al.* (2002) showing that the gravisensing may be more distributed in roots also]. Measurements of differential strain between the concave and the convex sides of the organ at the scale of a small element are the most closely responses that have been studied so far [see equation (5)]. Myers *et al.* (1995) did report such measurements at several initial stimulation angles and argued that they may not fit a sine law, but no dose–response characterizations have been produced. Insights from the cellular mechanisms determining graviperception and the bending response and their spatio-temporal distribution over the course of gravitropic stimulation and the gravitropic response may well prove informative on this point.

A brief overview of the molecular and cellular biology of gravisensing

The topic has been covered in detail in recent reviews (Kiss, 2000; Blancaflor and Masson, 2003; Haswell, 2003; Perbal and Driss-Ecole, 2003; Morita and Tasaka, 2004; Iino, 2006; Gilroy and Masson, 2008), and thus only the major features relevant from a biomechanical point of view will be summarized here, essentially for non-specialist readers. These features mainly involve two longstanding (though evolving) qualitative models: the 'starch-statolith' theory and the 'Cholodny–Went' theory.

The perception of gravity in aerial organs is localized in a specific tissue, the endodermis in dicot young stems and inflorescences and the starch-sheath in monocot pulvini (Morita and Tasaka, 2004) and woody stems (Nakamura *et al.*, 2001). These tissues have specialized cells called statocytes, usually containing large starch-filled plastids or amyloplasts. Mutants lacking proper endodermis differentiation are agravitropic (Tasaka *et al.*, 1999; Morita and Tasaka, 2004). Moreover, most of the perception of the dose and orientation of the gravitational stimulus in these cells is related to the downward movement of the amyloplasts, which thus function as statoliths. This downward movement would allow them to activate trans-membrane receptors, possibly mechanosensitive channels triggering Ca^{2+} influxes and $InsP_3$ amplification (Perbal and Driss Ecole, 2003; Valster and Blancaflor, 2008), and eventually switching on gene transduction.

Indeed, amyloplast mutants lacking starch or with reduced starch content display reduced gravitropic response, whereas mutants with excess starch display an enhanced response (Tanimoto *et al.*, 2008). By the same token, shoots with reduced starch content due to carbon starvation (i.e. dark or a deep shade) are also less responsive. Moreover, using a high-gradient magnetic field (HGMF) exerting a ponderomotive force on endogenous amyloplasts, Weise *et al.* (2000) were able to demonstrate that tropic curvature is induced locally in stems, i.e. only occurring in regions growing and displaying amyloplast displacement. HGMF-induced amyloplast displacement in the lignified basal part of the stem, for example, had no effect on tropic curvature. The perception of orientation versus gravity and of the corresponding dose of gravistimulation thus involves amyloplast movements in the direction of gravity, in accordance with the longstanding 'Starch-statolith' theory. Note, however, that mutants lacking downward amyloplast movements still display a weak gravitropic response, which suggests that amyloplast statoliths seem to be an evolutionary mechanism for amplifying gravisensitivity, in addition to a presumably ancient mechanism related to the direct sensing of protoplast pressure (Perbal and Driss Ecole, 2003).

The movement of the starch-filled statoliths does prove to be more complex than initially thought. The high density of starch compared to mean cytoplasmic content means their weight overcomes the buoyancy reaction and the viscoelastic friction of the cytoplasm, with the result that sedimentation can occur. However, amyloplast movement is clearly regulated by interactions with vacuoles and vacuole trafficking, especially in shoot statocytes (Morita and Tasaka, 2004; Saito *et al.*, 2005). Moreover, reports have cited a direct influence of the actin cytoskeleton and also of actin–myosin molecular motors (Palmieri *et al.*, 2007). Interestingly, it has been argued that the actin cytoskeleton may down-regulate gravitropism by continuously resetting the graviperceptive system and by controlling the signal-to-noise ratio (Morita and Taska, 2004; Palmieri *et al.*, 2007). This raises the important issue of putative accommodation of the sensitivity of the gravisensing system (LaMotte and Pickard, 2001; Moulia *et al.*, 2006). Indeed, it has been shown in roots that statocytes grown in microgravity are more sensitive than those grown on a 1 *g* centrifuge in space (Perbal and Driss-Ecole, 2003). This is consistent with older reports that clinostatted plants subsequently show increased graviresponses (Audus, 1969). This accommodation of gravisensitivity might be partially reflected by the logarithmic dependence of the macroscopic gravitropic response Ω_g on the stimulation dose S_d: $\Omega_g=\lambda_{(\gamma)}+\mu\log(S_d)$. Indeed, the increment of response $\partial\Omega_g$ due to an increment in the stimulation dose ∂S_d then becomes:

$$\partial\Omega_g = \frac{\mu}{S_d}\partial S_d \qquad (8)$$

so that sensitivity to a variation in the dose of the stimulus is inversely proportional to the current level of the stimulus, meaning very fast accommodation.

However, the model in equation (8) is likely to be insufficient (Perbal *et al.*, 2002) and the specific process of accommodation with its specific time scales will have to be given more in-depth analysis. By the same token, the molecular mechanisms underlying the modulation of the Gravity Setpoint Angle by development or environmental cues remain unknown.

More insights into the dynamics of amyloplast movements might come from the recent techniques of *in vivo*

imaging. In particular, the confocal imaging of the Pt-GFP transgenic line of *Arabidopsis* with its Green Fluorescent Protein expressed exclusively in the amyloplast of the endodermis (Palmieri *et al.*, 2007) should be particularly informative. It might also stimulate the new generation of formalized bio-physical modelling that is necessary to further our understanding of the dynamics of the gravisensing cell and to build systems biology models of graviperception (since the active modelling activity of the pioneers, including the elegant work by Audus, 1964, has unfortunately faded away). There is currently no cellular-based mechanistic model that could replace/improve phenomenological sine law for quantitative studies and integrative organ modelling.

The downward movement of amyloplasts, as sensed through mechanoreception, is thought to interact with the PIN3 auxin efflux transporter, which is located exclusively in the inner side of the endodermis and facilitates centripetal auxin efflux. This is likely to establish a link with the other major feature of the current view on gravitropism: the asymmetric radial polar transport of the plant hormone auxin (see Tanaka *et al.*, 2006, and Muday and Rahman, 2008, for recent reviews). Auxin moves along the stem to the root through a unique polarized transport mechanism involving several cellular influx and efflux transporters and, in particular, the specific localization of efflux transporters from the PIN and probably MDRP/PGP families.

This polar transport of auxin results in axial auxin gradients down the stem, peaking in the stem growth zone (Muday and Rahman, 2008). Upon gravistimulation, by reorientation and relocalization/activation of PIN3 auxin transporters (and/or other auxin transporters), a transverse (radial) gradient builds up across the stem, with peak auxin concentration in the lower side. This difference in concentration is supposed to drive the motors of the gavitropic response differentially. The literature now refers to this qualitative model as the 'Cholodny–Went hypothesis' (see, however, Firn and Digby, 1980, for a more informative historical view). Although the debate continues (Firn *et al.*, 1981), this hypothesis has received considerable support from radio-labelling, molecular and genetic studies (see Tanaka *et al.*, 2006; Du and Yamamoto, 2007; Muday and Rahman, 2008, for more detailed arguments). Philippar *et al.* (1999) used ultra-precise gas chromatography-mass spectroscopy (GC-MS) directly to quantify auxin concentrations in maize coleoptiles with high resolution. Upon gravistimulation, two changes in auxin gradients were observed (Fig. 7): (i) a rise in the longitudinal gradient with increased free auxin near the tip within 5–10 min, and (ii) after 15 min, the onset of a 'Cholodny–Went-like' up–down gradient, starting from the tip and proceeding down the coleoptile within 45 min. Unfortunately, there was no attempt to model these results mathematically. Moreover, this view may still be too simplistic. Indeed, the control of polarized auxin transport is much more dynamic than the classical description outlined above. It involves complex transporter endosome trafficking (again involving molecular actin–myosin motors) and feedbacks from auxin itself (plus other regulators, including ethylene and $InsP_3$, both of which are also associated with mechanotransduction, and others such as flavonoids). Moreover, the regulation of auxin sensitivity seems to be required for asymmetric gene expression (Salisbury and Ross, 1992) and auxin-dependent and auxin-independent pathways may co-exist (Yoshihara and Iino, 2007). Last but not least, some responses cannot be fully explained through the current 'Cholodny–Went' theory. For example, the dampened oscillations alternating bending and counter-bending that occur before reaching a stabilized vertical GSA position (Fig. 5) are not matched by preceding oscillations in auxin transport and across-organ concentration (Haga and Iino, 2006), although a steady asymmetric auxin gradient is required (Dolk, 1936). Bioassays, radiolabelling, and GC-MS analyses in tree stem with secondary growth and reaction wood-mediated gravitropism have yielded contradictory results as to the possible transverse gradients in auxin concentration, although the dominant, yet debated, view is that transverse gradients of auxin are involved in i) compression wood formation, in interactions with ethylene, and ii) possibly also in tension wood, in interaction with gibberellins. Nevertheless, a direct influence of bending perception *per se* (besides that of auxin gradients) is also involved (Du and Yamamoto, 2007).

Most of the recent reviews on gravitropism usually stop here. Some add a short paragraph on the action of auxin on cellular expansion, usually detailing some of the many downstream regulated genes. However, at this point, nothing has yet been said about 'the power of movement'! Indeed, power in science has a clear meaning: the time-rate of delivering free energy, by doing work for example (it is likely that this thermodynamics-based meaning of power

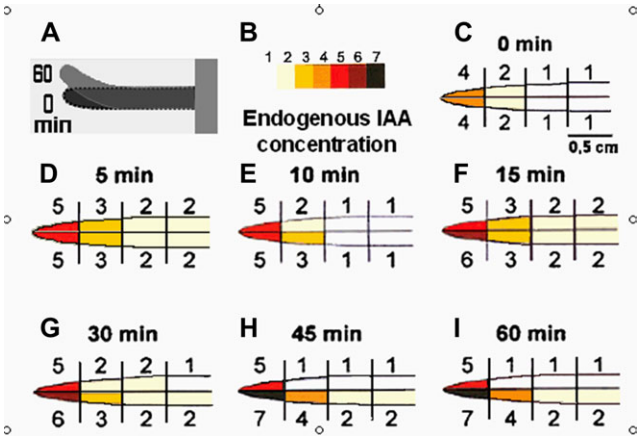

Fig. 7. Redistribution of endogenous auxin (indole acetic acid, IAA) concentrations during the early phase of the gravitropic movement of coleoptiles in response to a 90° gravi-stimulation (see also Fig. 1B). (A) Gravitropic movement between 0 min and 60 min; (B) IAA concentration (pg IAA mg^{-1} fresh weight) in 0.5 cm segments of coleoptile halves decomposed into seven concentration ranges and colour-coded; (C, D) endogenous IAA concentrations in coleoptiles gravi-stimulated for 0, 5, 10, 15, 30, 45, and 60 min (from Philippar *et al.*, 1999, © National Academy of Sciences, USA).

was prevalent in the Darwins' mind when they wrote their book, as Joule and Helmholtz's works dates back to the 1840s, but we leave this point to the historians of Science). Power has its SI unit Joules per second (or Watts), and is also expressible as the product of the force applied to move an object and the velocity of the object in the direction of the force (Power, 2008). The power of movements would thus measure a flux of free energy that is necessary to bend the organ and to move it back to its GSA. Understanding the power of movement thus requires a response to questions of the motors involved and the resistances to this active movement. Furthermore, as gravitropic bending is a whole-organ response, the cellular level is not enough. How are organ anatomy and morphology related to the rate of curvature change $D\kappa_{(s,t)}/Dt$ and to the changes in tip angle?

The power of tropic movement: motors and resistances

A motor is a device that transforms some potential free energy into work (at a time-rate characterizing its power). At the cellular level, plants have two major motors (Moulia *et al.*, 2006). The first one is an osmo-hydraulic motor (OsmH motor; Fig. 8A1) and is found in cells with primary cell walls. The second is a polymeric swelling/shrinkage motor (PSS motor; Fig. 8B1), and is found in cells with secondary cell walls.

A resistance is a biophysical process that counteracts the motor system by absorbing part of the free energy, either by storing it in a potential form that cannot be used for producing the movement (e.g. blocking of the gravitropic movement by a stiff stake storing elastic energy out of the gravitropic organ; Yamashita *et al.*, 2007; Ikushima *et al.*, 2008) or by dissipating this free energy into heat (a degraded form of energy) through some friction. There are two types of resistances: those internal to the motor (reducing its energetic efficiency) and those external.

Osmo-hydraulic motors

Osmo-hydraulic motors can be found in apical growth zones of stems and roots, and in intercalary primary growth zones such as grass pulvini or grass blade joints (Moulia *et al.*, 2006). Their major features are summarized in another long-standing model, that of Lockhart (Lockhart, 1965; see review in Tomos *et al.*, 1989; Ortega, 1994; and see Dumais *et al.*, 2006, for the most recent update, although applied to the case of tip growth). Lockhart's model was set up in the 1960s after several decades of physiological research starting with Pfeffer's work in 1877 (discussed by the Darwins in 'The power of movement', see also Pfeffer, 2008, in *Encyclopaedia Britannica*); but the advance brought by Lockhart was to turn a qualitative hypothesis into a quantitative biophysical structure–function model. As plant cells are surrounded by a stiff cell wall and the deposition of cell wall polymers occurs at the interface between the inner face of the cell wall and the plasma membrane (Johansen *et al.*, 2006), the irreversible changes in length during growth require a cell wall able to stretch irreversibly over time, i.e. displaying creep (Fig. 8A1). This creep can be measured by the time-rate of change of its relative length, i.e. the growth-induced longitudinal strain rate $\dot{\epsilon}_{(s,t)}$ (as defined in the section about kinematics). It has been experimentally demonstrated that the work required for this irreversible stretching involves longitudinal stresses in the cell-wall σ. These stresses represent internal forces per unit surface area (units MPa) acting longitudinally within the cell wall (there are in fact stresses acting in all three directions, but only the longitudinal component works towards elongation here). They arise from the reaction of the cell wall to the turgor pressure P of the cell, as well as to any external loads σ_{ext} from neighbouring cells or from the environment (external loads are expressed as the resulting force per unit cross-sectional area of the tissue σ_{ext} to keep them harmonized with turgor pressure P). Creep only occurs after a minimal stress or (plastic) yield threshold σ_y has been reached, and permanent work is required to maintain a given strain rate $\dot{\epsilon}_{(s,t)}$ due to the viscoplastic resistance of the cell wall itself, which dissipates part of the work into heat. Moreover, elastic cell stretching may occur in response to changes in turgor pressure or external load. By setting a biomechanical model based on minimal parameterization of this anisotropic visco-elasto-plastic cell wall behaviour, and resolving the mechanical equilibrium for a cylindrical cell with longitudinal extension only (anisotropic growth), the previous description of the experimental results can be summarized into the following equation (Ortega, 1994):

$$\dot{\epsilon}_{(t)} = \frac{1}{\Phi^{-1}_{(t)}}\left(P_{(t)} + \sigma_{ext(t)} - P_{Y_{(t)}}\right) + \frac{1}{E}\left(\dot{P}_{(t)} + \dot{\sigma}_{ext(t)}\right) \quad (9)$$

Strain rate — viscoplastic = growth — elastic = reversible

where $\dot{\epsilon}_{(s,t)}$ is the longitudinal strain rate, P is the turgor pressure, σ_{ext} is the external longitudinal stress, $\dot{P}$ and $\dot{\sigma}_{ext}$ are time-rate of change in P and σ_{ext}, P_Y, Φ, and E are global cell mechanical properties (see details below). Note that the P and σ variables must be expressed in the same unit (for example, MPa).

This equation means that power from turgor pressure P and, eventually, neighbouring cells σ_{ext} is required for the cell wall extension to overcome two types of internal resistances: visco-plastic extension of the cell wall, and the housing of potential elastic energy into the cell wall.

The visco-plastic creep is the irreversible growth component found in growing cells; it is characterized by two parameters P_Y and Φ. P_Y is the pressure (and/or any external forces per unit surface over the entire cell) required to reach the plastic yield point of the cell, Φ is the visco-plastic extensibility of the cell in relation to the rheological processes in the cell wall (internal frictions and bound ruptures) and to the relative thickness of the cell wall versus cell radius; Φ^{-1}, its inverse, is the visco-plastic resistance of the cell.

The elastic extension is a reversible term (i.e. it can be recovered upon de-loading, such as through plasmolysis, provided there

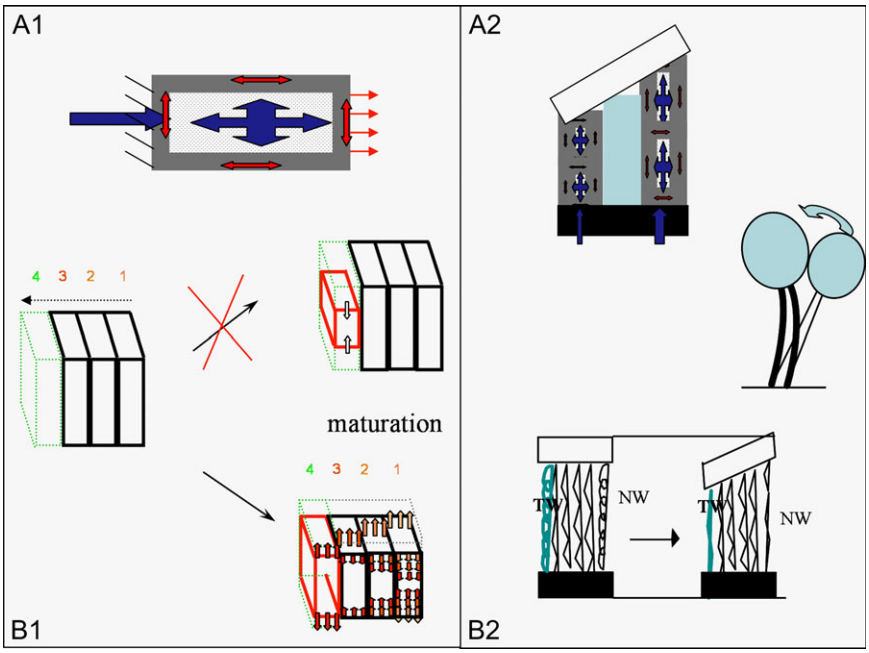

Fig. 8. The two basic types of motors producing mechanical work, deformation and movements in plants, at cell level (left) and at organ segment level (right). (A) Hydraulic motors in primary (non-woody) tissues: (A1) diagram of a cell showing the reversible or irreversible stretching of the cell wall under hydrostatic (turgor) pressure due to internal osmotic potential and possible external stresses. The cross-arrow inside the cell sketches out internal hydrostatic pressure. This hydrostatic pressure and the external stresses are balanced by internal stresses (arrows) in the cell wall that result from the mechanical stiffness of the cell wall under stretching. A water flux enters the cell (left arrow) due to differences in water potential between the inside and the outside of the cell. This difference provides the free energy for the work of cell-wall stretching. If elastic stretching occurs, then this energy is stored as potential elastic energy in the cell wall. If irreversible stretching (growth) occurs, then part of this energy is dissipated by the cell wall viscosity (A2); if the hydraulic stretching of cells is heterogeneous across the cross-section of the stem, active bending occurs. (B) Cumulative shrinkage/swelling motors in secondary woody tissues (illustrated here in angiosperms): (B1) diagram showing the motor effects of the addition of an outer cell layer (4) produced by secondary growth (dashed arrow) to older layers (1 to 3) and the cell-wall differentiation (maturation) of this outer layer (4). With polymerization in the secondary cell wall, the maturing new cell layer tends to shrink longitudinally (drawing at top). However, this maturation shrinkage is not possible, as it is limited by older layers (drawing at bottom). The new cell layer is thus put into a state of tension (external arrows), whereas the inner layers (that were initially in tension due to their own maturation shrinkage) experience an increment in compression (internal arrows). As the process is reiterated with new layers, successive compressions accumulate (additional arrows indicate accumulating compression stresses). (B2) If this shrinkage is heterogeneous across the cross-section of the stem (such as when tension wood is produced), then active stem bending occurs. (Adapted from Moulia *et al.*, 2006, and reproduced by kind permission of the Botanical Society of America.) (TW, tension wood; NW, normal wood.)

have not been too many cell wall deposition; Peters and Tomos, 2000). It can be found in all the cells, and is characterized in this simple model by one parameter, E, which is the bulk elastic stiffness of the cell wall in relation to the mean elastic stiffness of the cell wall material (its Young's modulus) and to the relative thickness of the cell wall versus cell radius.

In cells undergoing steady growth conditions ($\dot{P}$ and $\dot{\sigma}_{ext} \approx 0$) with no external load ($\sigma_{ext} \approx 0$), cells may grow typically at $\dot{\epsilon}_{(s,t)}=1\%\ h^{-1}$ in stems (Girousse *et al.*, 2005). In tissues undergoing steady growth, P is typically $\approx$0.5 MPa (Tomos *et al.*, 1989). Assuming a yield threshold of around 0.25 MPa, the visco-plastic resistance of the cell wall Φ^{-1}comes to 25 MPa h, meaning that 25 MPa above the yield threshold, i.e. 250 bars (!), would be required to double the size of the cell every hour, working against cell wall resistance (this is probably exceeding the wall strength though).

In natural (non-steady) conditions, all the parameters in equation (9) may change with time and thus have a (t) index. These changes are usually under biological control. However, the only biological controls that are relevant for gravitropism are those differentially expressed between the concave and convex sides during gravitropic movement (Fig. 8A2; Tomos *et al.*, 1989; Cosgrove, 1990*b*). The visco-plastic resistance of the cell wall decreases quickly with auxin, at least in the epidermal outer cell wall (see Kutschera and Niklas, 2007 for a review). This is probably due to cell wall acidification triggering expansin-dependent weakening of hydrogen bonds and, in the longer term, to auxin-induced expression of expansin (Muday and Rahman, 2008, but see counter-arguments in Ikushima *et al.*, 2008). Differential changes in pectin and xyloglucan polymer size in the upper and lower parts of bean epicotyls also correlates to differential changes in wall extensibility as a response to inclination, and not bending (Ikushima *et al*,. 2008). Such changes may also be triggered by auxin through the induction of xyloglucan endo-transglucosylase/hydrolase (XTH), and/or changes in

exocytotic rate of matrix polymer deposition (see Ikushima *et al.*, 2008, for a review). Note that it is bending, but not inclination angle, that has been shown to induce differential changes in the cortical microtubules (MT) between the upper and lower epidermis during gravitropic movement. MT orientation is usually related to the orientation of the 'extrusion' of cellulose microfibrils in the cell wall and thus to cell-wall extensibility (Ikushima and Shimmen, 2005), providing evidence for the involvement of a mechanoperceptive control over bending rate in gravitropism (independently of auxin and of inclination sensing).

As highlighted by the Darwins (1880), differential pressure in the upper and lower part is also a candidate explanation for differential growth during tropisms. However, direct measurements using cellular pressure probes demonstrate that, although changes in pressure do induce changes in strain rate in plants, no significant difference in pressure has been observed between the upper and lower parts of graviresponding organs (Tomos *et al.*, 1989; Cosgrove, 1990*b*, Kutschera and Niklas, 2007; Ikushima *et al.*, 2008).

However, cell wall yielding under pressure is not sufficient to understand cell growth fully. The increased cell volume is filled with water (so no vacuum can occur), meaning that water influx needs to be coupled with pressure-driven expansion (Fig. 8A1). This is likely to occur through passive water flow. The power for this influx is related to the gradient in the water potential Ψ between the interior of the cell and the water source (the water potential is the amount of work that would be necessary to bring a unit volume of water back into a reference state of free water at atmospheric pressure and constant temperature; Ψ is by convention a negative, and its unit of expression is MPa). This kind of gradient exists because an osmotic potential, $-\Pi_i$, is maintained within the cell. The resistance R_h to this water flow is due to water pathway-long 'frictions'. This includes the hydraulic resistance not only of the cell membrane but also throughout the path of water flow from the source to the growing cell (Tomos *et al.*, 1989). This can be stated in the second Lockhart equation:

$$\dot{\varepsilon}_{(t)} = \frac{1}{R_{h(t)}} \cdot \left(\left(P_{ext(t)} - P_{(t)} \right) - r\left(\Pi_{ext(t)} - \Pi_{i(t)} \right) \right) \qquad (10)$$

where P_{ext} is the pressure of the external water source, P is the internal turgor pressure, r is the reflection coefficient of the membrane (a parameter ranging from 0 to 1 and measuring the degree of hemipermeability, 1=permeable only to water), $-\Pi_{ext}$ is its osmotic potential (i.e. Π_{ext} is its osmotic pressure), and (P_{ext}–Π_{ext}) is the water potential Ψ_{ext} of the external source, R_h is the integrated resistance to water flow. Equation (10) says that the growth-induced strain rate depends on the differences between hydrostatic and osmotic pressures in the external source and inside the cell. The water pathway and thus its integrated resistance R_h can vary significantly within the same organ depending on whether it grows in air or in water (e.g. submerged versus air-grown rice coleoptiles, see Fig. 3, or aeroponic roots versus hydroponic roots). But resistance along the water pathway is not the only source of resistance to water influx. A lower Ψ_{ext} (i.e. small P_{ext} and/or large osmotic content Π_{ext}) results in less water available for growth (as is the case during water stresses). In addition, equation (10) shows that a high turgor pressure P tends to squeeze water out of the cell. Thus turgor pressure has an opposite effect in equations (9) and (10).

Actually, equation (10) is insufficient. Water influx is only possible if the internal water potential is actively and biologically maintained by adjustments of the internal osmotic potential $-\Pi_i$ of the cell and by the maintenance of the cell's (almost) hemipermeable membranes (both involving consumption of metabolic energy). Although rarely cited in reviews, this leads to a third equation expressing the changes in internal osmotic potential $-\Pi_I$ (assuming the Van't Hoff equation for osmotic pressure in diluted solutions, and neglecting Onsager's coupling between passive water and ionic fluxes , i.e. r=1; see Boyer and Silk, 2004):

$$\frac{d\Pi_{i(t)}}{\Pi_{i(t)}dt} = \frac{1}{n}\left(\frac{dn}{dt}\right) - \frac{1}{V}\left(\frac{dV}{dt}\right) = \frac{1}{n}\left(\frac{dn}{dt}\right) - \dot{\epsilon} \qquad (11)$$

Osmotic adjustment; Dilution by water flux; Growth-induced strain rate

where n is the number of osmoles in the cell vacuole and V is the cell volume.

Equation (11) just states that osmotic adjustment by changing the number of osmoles n has to match the dilution by water influx due to the growth-induced strain rate in order for the osmotic pressure to be maintained and for the osmohydraulic motor to maintain steady work. This adjustment is thought to involve strain or strain-rate mechanosensing by mechanosensitive channels (Telewski, 2006), which makes sense from equation (11). It may involve membrane transporters actively pumping (i) ions (e.g. potassium K^+) from the surrounding apoplast, (ii) amino acids arriving from phloem downloading (e.g. proline), as well as the hydrolysis of polymers into monomers, for example, starch from amyloplasts (Tomos *et al.*, 1989). It is thus a complex phenomenon requiring the supply of free energy and a tuned control through sensing.

There has been a wave of interest into osmotic adjustment, water relations, and gravitropism since Philippar *et al.* (1999) reported that the gene coding for the inward potassium channel ZMK1, and presumably involved in the osmotic adjustment term dn/dt in equation (11), was an Aux-RE primary auxin response gene. Moreover, ZMK1 differential expression between the upper and lower sides of a gravireacting coleoptile led to increased K^+ channel density *in vivo*. Some commentators (but not the authors) then wrote 'Moving on up: auxin-induced K^+ channel expression regulates gravitropism' (Bennett *et al.*, 2000). Miyamoto *et al.* (2005) also demonstrated in aeroponically growing root that the resistance to the water pathway R_h was much smaller in the rapidly expanding side, thus modifying the growth-induced strain rate according to equation (10), although they could not establish the link with increasing density of the aquaporin

water channels. However, it is not physically possible to consider any of the three above-cited equations alone. They are coupled and have to be considered together as a three-equation system, i.e. the Lockhart model. Wall visco-plastic resistance to stretch in equation (9) may overcome the effects of changes in resistance to water influx or even reduce the effect of osmotic changes. Only considering the three-equation system can give insights on the effect of gene expression on some parameters. The effect of this change might be minute or compensated by changes in other parameters. This is not to say that osmotic control is unimportant. Indeed, in the absence of a model for osmotic adjustment, Lockhart (1965) considered two extreme cases of osmoregulation: either a perfect and immediate osmotic adjustment

$$\frac{d\Pi_{i(t)}}{\Pi_{i(t)}dt} = 0 \Rightarrow \frac{1}{n}\left(\frac{dn}{dt}\right) = \frac{1}{V}\left(\frac{dV}{dt}\right)$$

or the absence of any adjustment

$$\frac{1}{n}\left(\frac{dn}{dt}\right) = 0 \Rightarrow \frac{d\Pi_{i(t)}}{\Pi_{i(t)}dt} = -\frac{1}{V}\left(\frac{dV}{dt}\right)$$

He then went on to show that, in the absence of osmotic regulation, growth vanished rapidly whatever the cell-wall properties. Primary elongation is a fully-fledged osmotic motor. However, the Lockhart model may also be used to show that a much more efficient strategy is to co-regulate several parameters simultaneously, for example, through transcription factors (e.g. ARFs). It remains striking that several authors have found no differences in osmotic pressure (nor turgor pressure) between the two sides of gravireacting organs, thus indicating that the regulation of osmotic pressure and of cell-wall properties might have been tuned together. The Lockhart model can, as a tool, go beyond the correlative arguments between (i) the expression of a single gene (although many others have probably varied as well, e.g. expansins, since many early transcriptional and post-transcriptional changes have been described; see Harisson *et al.*, 2008), (ii) differential changes in one parameter, and the overall effect of growth. Analysing the (non-additive) effects of variations on the parameters in the model can provide insights into their relative degree of control. However, the Lockhart model only works at the scale of one cell, whereas we know that gravitropic bending involves the complete organ. What is needed is a model working at least at organ-segment level.

Polymeric swelling/shrinkage motors

Schematically, growing cell walls are made of polymers and water. Wall polymers are formed by (i) the partly crystalline cellulose microfibrils (the stiffest component) and (ii) hemicelluloses, Ca^{2+}-pectin gels and proteins making up the matrix. Once expansion growth has stopped, some cells have an additional group of phenolic polymers that polymerize *in situ* in the cell wall and function like a hydrophobic glue: the lignins (see Mellerowicz and Sundberg, 2008, for a recent update on the complexity of this issue). Moreover, even after expansion growth has ceased, layers of cell wall may continue deposition. These cell wall layers are thus called the secondary wall, and the process of final differentiation of this secondary cell-wall is called maturation. Secondary cell-wall layers are particularly thick in fibre cells, which can be found either in primary tissues after the cessation of growth (sclerenchyma) or in the secondary woody tissues produced by the cambium. During polymerization, any material changes size spontaneously, either displaying swelling or shrinkage, meaning that its rest (unloaded) size also changes. Such spontaneous changes in the rest size are clearly observed during cell-wall maturation (Archer, 1987) although the molecular mechanism generating dimensional variations of the cell wall material is still a matter of debate (especially concerning the role of crystallinity in cellulose microfibrils, see Burgert *et al.*, 2007; Clair *et al.*, 2007).

Longitudinal shrinkages thus occur during cell-wall maturation in normal wood fibres (Fournier *et al.*, 2006) and probably also in sclerenchyma cells (Hay *et al.*, 2000). However, evolution has progressively selected two special types of fibres in tissues called reaction woods (Fig. 8B1). These reaction woods present distinct longitudinal changes in size upon maturation (Mosbrugger, 1990) and have been classified as tension wood or compression wood. Tension wood (TW) is found in most dicotyledons with secondary growth, including trees but also herbs (Patten *et al.*, 2007). TW is characterized biomechanically by an increased longitudinal shrinkage upon normal wood (NW). If restrained longitudinally by other tissues, TW thus tends to enter into a tension state by pulling on the adjacent tissues (Fig. 8B2). CW displays a longitudinal swelling during cell wall maturation. If restrained longitudinally by other tissues, CW thus tends to enter into a compression state by pushing up the adjacent tissues. CW is typically found in conifers and in some species of the basal lineage of the angiosperm eudicot *Buxus*. Swelling woods have also been reported to form in the opposite side of stems producing TW in angiosperms (Clair *et al.*, 2006). Reaction wood is thus neither a trait of recent seed plants nor a particularity of a few taxons. It has been described in all plants with a cambium (Mosbrugger, 1990), even in the most ancestral trees such as the late Devonian progymnosperm *Archaeopteris* (Scheckler, 2002). Longitudinal shrinkage and swelling can be characterized by the relative change in length or longitudinal strain due to maturation ε_m. Within the framework of elastic theory, the stress generated at maturation in the longitudinal direction can thus be written

$$\sigma_{(x,y,s)} = E_{(x,y,s)}\left(\varepsilon_{(x,y,s)} - \varepsilon_{m(x,y,s)}\Delta m_{(x,y,s,t)}\right) \qquad (12)$$

where σ is the longitudinal stress, x and y characterize the position within the cross-section of the organ, s is the distance along the organ, E is the longitudinal Young's modulus of elasticity (stiffness of the woody material subjected to a reversible longitudinal stretch, in MPa units), ε_m is the maturation strain (that would occur in

the material if free of any mechanical restraint), and $\Delta m_{(x,y,s,t)}$ represents the changes in the state of the polymers comprizing the cell wall during maturation (from 0 in the cambium to 1 in the cells with fully-mature secondary cell wall). A higher E and a higher ε_m (either positive or negative) will mean more work can be produced. Just as with differential growth, it is possible to measure the difference in maturation strains ε_m between the upper and the lower side of a gravireacting organ (Fournier *et al.*, 2006), i.e.

$$\Delta\varepsilon_{m(s)} = \left(\varepsilon_{m(s,t,-w/2)} - \varepsilon_{m(s,t,+w/2)}\right) \quad (13)$$

where w is the width of the organ in the plane of curvature [see equation (4)]. Note that $\Delta\varepsilon_m$ is often noted α or $\Delta\alpha$ in the literature (e.g. Archer, 1987) but $\Delta\varepsilon_m$ was preferred here for the purposes of consistency and to avoid confusion with inclination angle α).

Maturation strain ε_m has been estimated experimentally by locally releasing the stresses (Yoshida and Okuyama, 2002; Fournier *et al.*, 1994*b*). It was found to display a broad range of values in woody species ranging between –0.5% (severe shrinkage in strong TW) to +0.3% (severe swelling in strong CW), meaning that large differences in the power of the PPS motor can be expected (Fournier *et al.*, 1994*b*; Archer, 1987).

Just as for primary growing cells, structure–function models have been designed to relate E and ε_m to the geometry of the fibre cell and the mechanical properties and orientation of the components of its cell wall (e.g cellulose microfibrils; see Archer, 1987). However, the fact that the cell wall anisotropy has to be considered in more detail means expression is mathematically more complex than in the Lockhart model, and will not be presented here. The major parameter influencing ε_m is the angle between the cellulose microfibrils (MFA) and the longitudinal axis of the cell. In TW, for example, the smaller this angle (i.e. the more longitudinal the microfibrils), the higher the ε_m and E and thus the more powerful is the TW. Very little is known about the biological control of MFA, but cytoskeleton changes in relation to orientation versus gravity, auxins, and direct bending sensing are all likely to be involved (Du and Yamamoto, 2007). Consequently, the osmo-hydraulic motors and the polymeric swelling/shrinkage motors might share similar gravisensitive controls (but this remains to be studied in more detail). Note, however, that although cell maturation occurs while the cell is still living, turgor pressure or its variations are not involved in the generation of maturation strains (Almeras *et al.*, 2006).

In contrast with osmo-hydraulic motors, the polymeric swelling/shrinkage motors are not continuous over time at the cellular level. The maturation deformation happens only once during the life of a fibre cell (just before apoptosis). Any one cell is just producing one increment of motor activity. However, differentiating fibres are produced continuously downstream of meristems (Hay *et al.*, 2000; Fournier *et al.*, 2006), so that new PSS motor increments are continuously being added at the level of the growing organ. Hence, if DR/Dt is the rate of addition of new layers of maturating cells in the organ (the following only considers the case of cambial secondary growth), then the time-rate of motor input at position s and time t could be $\Delta\varepsilon_m DR/Dt$. However, active bending during gravitropism involves many different cells with different positions in the cross-section. What about the effective power of the motor cells at the cross-section level? We will see that this includes much more than the time-rate of motor activity.

The conflict between motors and internal resistances at organ cross-section level: autostresses and bending power

As the cross-section of gravireacting organs comprises numerous cells of different tissues, the question arises as to whether or not all the cells are producing co-ordinated motor activity right across the organ. This question is easy to assess experimentally by mechanically disrupting the continuity of the organ, such as by making a notch by cutting the organ into pieces with a razor blade or a saw. If it takes work to fit the pieces back together, then there have been internal forces occurring in the intact organs between cells and tissues. While the structure of the organ was intact, these internal tissue-stresses balanced themselves out, which is why Solid Mechanics uses the term autostresses, for auto-equilibrated stresses. These autostresses are produced from incompatibility in the at-rest shape of the components within the structure of the organ itself (Moulia, 2000). In mechanical engineering, autostresses are also called 'pre-stresses' as they usually arise before use, when manufacturing mechanical systems. However, this is a misnomer in biological systems, which produce autostresses continuously throughout their lifetime. Autostresses are a generic feature of all growing systems, animals, fungi, and plants (Hejnowicz, 1997; Moulia, 2000; Sharon *et al.*, 2002; Ben Amar and Goriely, 2005; Fournier *et al.*, 2006; Moulia *et al.*, 2006). In botany, they were first identified in the 19th century by Hopfmeister as (i) tissue tensions or tissue stresses in non-woody tissues (see Peters and Tomos, 1996, and Kutschera and Niklas, 2007, for historical reviews), and (ii) growth stresses (Archer, 1987) or maturation stresses in woody tissue (reviewed in Fournier *et al.*, 2006). Figure 9 shows two examples of end-split stems [herbaceous stem (A), (B), and a woody stem (C)] displaying clear shape changes after notch opening.

What are the consequences of autostresses for the power of bending organs? In plant tissues, as previously stated, the cells are tightly glued together by a very thin middle lamella. Consequently, the Bernoulli hypothesis of beam/rod theory stating that an imaginary cross-section would remain planar along bending proves correct (as long as the curvature is not too high, or more precisely, as long as its inverse, the radius of curvature, is much larger than organ width w). This is easy to assess by drawing a circular mark around a gravireacting organ and seeing it remain in the same plane across the organ during bending. This actually forms the basis of the marking experiments in Fig. 4 [and

equations (4) and (5)]. A more quantitative validation of beam theory using composite mechanics in plant organs can also be found in Moulia and Fournier (1997). Auto-equilibrium means tissue stresses can be balanced without an external load. Therefore, the sum of all the longitudinal stresses acting on a given cross-section CS(s) is zero:

$$\int_x \int_y \sigma_{(x,y,s))} \cdot dx \cdot dy = 0 \qquad (14)$$

Moreover, in gravitropism, the forces involved are not only the sum of autostresses but also the sum of autostress-generated internal bending moments (Fig. 9D). These bending moments are produced by autostresses through their internal lever-arm (i.e. on its distance from the centre of bending y), giving

$$\int_x \int_y \left(\sigma_{(x,y,s))} \cdot y\right) \cdot dx \cdot dy = 0 \qquad (14b)$$

The longitudinal extension is driven by equation (14) whereas the active bending is mostly driven by equation 14b (see Almeras and Fournier, 2008, for more details). Both are dependent on the mechanical properties of extension at the tissue level as well as on the geometry/anatomy of the cross-section of the organ (and for the case of a primary growing tissue, on boundary conditions in terms of water potential, see equations (9), (10), and (11)).

Let's start with woody organs, as the situation is not controversial and has thus yielded a widely accepted biomechanical model. As seen from equation (12), wood can at first be considered as elastic. Indeed, upon splitting, it springs apart rapidly, giving direct evidence of auto-stresses (Fig. 9C). Moreover, the maturation strain of a given fibre cell only occurs once at a certain radial distance from the outside cambium. Each increment added in the radius of the maturated tissues DR triggers a maturation strain. But inner (older) cells to which the new maturating cells are glued tend to resist this maturation strain (Fig. 9). If, for example, the maturation strain is shrinkage, such as in TW, the inner core will be compressed. Equation (14) defines the mean increment in longitudinal strain $D\varepsilon_{(s,t)}$ due to an increment of radius DR of the maturing tissue ($D\varepsilon_{(s,t)}$ is minute as soon as $DR << R$). However, if the maturation strain is not axially symmetrical (e.g. where TW is only differentiated in the upper side of the stem), then there will be internal bending (Fig. 9). Assuming a sinusoidal variation of maturation strain around the circumference, and with mechanical equilibrium resolved, Almeras and Fournier (2008) found that for an increment in radius DR, the change in curvature $D\kappa$ is:

$$\frac{D\kappa_{(s,t)}}{Dt} = \Delta\varepsilon_{m(s,t)} \frac{DR_{(s,t)}}{Dt} \frac{2f_{(s,t)}\left(\bar{E}_{in(s,t)}/E_{out(s,t)}\right)}{R^2_{(s,t)}} \qquad (15)$$

where $\bar{E}_{in}/E_{out}$ is the ratio of the mean inner wood stiffness to the outer wood stiffness, f is a form factor that describes the angular distribution of growth and wood properties (f=1 if the cross-section is circular and concentric), and R is the radius of the cross-section. This model generalizes a previous version in Fournier *et al.* (1994*a*). Experimental studies (Almeras *et al.*, 2004; Coutand *et al.*, 2007) have demonstrated that this model offered fairly good predictions as long as the axis is not too slim and the time-scale used is around the level of months.

The important message of equation (15) is that, due to the internal resistance of the inner (older) tissue, the gravitropic response depends not only on the time-rate of motor activity at position s and time t, which is $\Delta\varepsilon_m DR/Dt$, but also on whole-organ anatomy, geometry, and size. Size effects are actually very important, as the increment in curvature is inversely proportional to the square of the radius of the inner tissues. Thus, for the same incremental

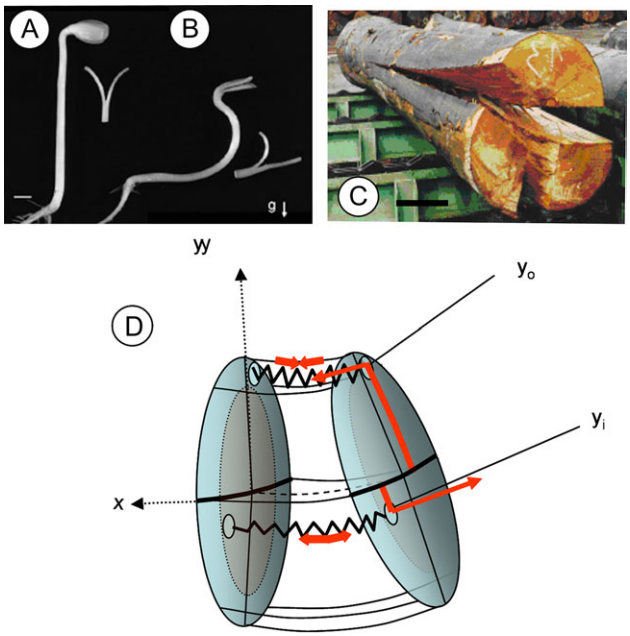

Fig. 9. Autostresses in growing stems. (A, B) Hypocotyl segments were split longitudinally and placed for 1 h in water; these segments were cut from a 4-d-old etiolated sunflower (A) grown vertically or (B) placed for 3 h in a horizontal position to induce gravitropic upward bending. Scale bar=5 mm (adapted from Kutschera and Niklas, 2007, reprinted from the *Journal of Plant Physiology* © 2007 with kind permission from Elsevier). (C) Tree trunk that automatically splits after being cut, even if not left to dry; scale bar=30 cm. (D) Internal lever arms for autostresses and the generation of active bending moment. In this example, the outer tissue tends to shrink (such as in tension wood) whereas the internal tissue shrinks less and is therefore stretched or, alternatively, the inner tissues tend to expand more than the outer tissue (such as in primary growing tissues). The external autostress acts with an internal lever-arm y_o that is much larger that the internal lever-arm y_i of the inner autostress. If no external bending moment is applied, the overall segment is in equilibrium, i.e. the integral (i.e. the sum) of the autostresses $\sigma(x,y)$ multiplied by their internal lever-arms y over the cross-section x y is zero. If this autostressed segment was split longitudinally, it would tend to open, as in (A), (B), and (C).

amount of maturation strain and the same amount of new maturating tissue, if the radius of the inner tissue is twice as big, the increment in curvature is divided by four for a given width of new maturating tissue (same dR) and by eight for a given amount of new tissue (same area $2\Pi RdR$)!

In the case of primary growing tissue, where each cell behaves as an osmo-hydraulic motor with the growth-related viscous terms incorporated in the system of equations (9), (10), and (11) of the Lockhart model, the situation becomes more complex. The open question is whether the external epidermal wall, which is approximately 5–10 times thicker than the wall of inner cells, restricts the longitudinal growth-induced strain-rate. This would mean that the turgor pressure of inner cells would not be fully borne by their own wall, and would thus add internal tensile forces to the outer epidermal wall (Kutschera and Niklas, 2007), thereby increasing the efficiency of the motor. According to equation (9), this would mean that σ_{ext} would be negative for inner cells and positive for outer cells (although in both cell types, the wall stress is positive due to the action of internal turgor pressures of the cell generally exceeding compressive σ_{ext}.). Compared with the situation with secondary growth gravitropism, here the core would be providing an additional push rather than resisting circumferential effects, while the epidermal wall would be controlling this push (Fig. 9A, B, D). These considerations gave rise to the 'epidermal-growth-control theory', which received interest due to the fact that auxins had long-since been shown to affect the expansibility of the outer layer—one of the early bioassays of auxin concentration, called Went's Pea test, was based on this fact—whereas brassinosteroids (another class of growth-controlling plant hormones) were recently shown specifically to affect the outer epidermis (see Kutschera and Niklas, 2007; Kutschera, 2008, for reviews). However, the immediate elastic component of the tissues is usually small (and may be related to the release of to so-called 'Poisson effects'; Hejnowicz, 1997). All the other strains require coupling between cell wall strain and water intake [equations (9) and (10)] and are thus time-dependent. By the same token, osmotic adjustment is likely to take place, as well as fast cell control of mechanical cell-wall properties (Peters and Tomos, 2000). In short, this is a complex problem, with controversial arguments (Peters and Tomos, 2000; Passioura and Boyer, 2003; Kutschera and Niklas, 2007; Kutschera, 2008), and would require a specific review. From a gravitropic perspective, however, it can be summarized by stating that contrary to secondary growth, there is no biomechanical model currently available that is capable of explaining the motor effects involved in active bending by differential growth at organ cross-section level. A key sticking point is that the level of dependence on organ diameter (and possibly on the thickness of the outer layer) is thus still unknown.

Lifting up weights and not getting fixed

Apart from the internal resistances to bending within the cross-section of the segment of an organ, two other resistances can act externally to the local gravitropic motor. One is external to the plant; the other is due to the weight of the other part of the plant (i.e. internal to the plant but external to the motor process itself).

Obviously, any contour force or constraints on the organ would affect active bending. This is the great difference between roots and shoots. The typical radius of free space in soils might have been a selective pressure driving selection for short-apical-growth zones in roots with tip-based graviperception. Note, incidentally, that contour forces are drastically different between a root in soil, a root in a hydroponic solution providing buoyant support and negligible viscous resistance, and an aeroponically grown root. This also applies to the comparison between gravitropism in air-grown rice coleoptiles and submerged rice (Iino *et al.*, 1996; see Fig. 6).

The other source of resistance is due to self-weight, namely the work required to lift the plant's weights. This depends on the mass distribution along the organ. As the corresponding weights act as bending moments, the lever arms between the weights and the point of active bending are also important. Moreover, masses and their related lever arms changes continuously with growth, making the related changes in self-weight bending moment important (see Almeras *et al.*, 2004, for an assessment of their relative importance in tree branches over development). These resistances due to self-weight and growth can be summarized as (Fournier *et al.*, 2006):

$$D\kappa_{(s,t)} = \frac{4}{\Pi} \cdot \frac{D\left(W_{(s,t)} \cdot H_{G(s,t)} \sin\gamma_{(s,t)}\right)}{E_{(s,t)} \cdot R^4_{(s,t)}} \qquad (16)$$

where $D\kappa$ is the material differential of curvature, W is weight above the cross-section, H_G is the distance from the centre of mass to the cross-section, γ is the leaning angle, $W_{(s,t)}H_{G(s,t)}\sin\gamma_{(s,t)}$ is the bending moment acting on the cross-section s, E is theYoung's modulus (i.e. the mean elastic stiffness of the tissues), R is the radius of the cross-section at position s, and $\frac{E_{(s,t)}\Pi R^4_{(s,t)}}{4}$ is the local flexural rigidity of the organ (for a mechanical model of the bending rigidity of a more complex anatomy-based cross-section, see Moulia and Fournier, 1997; Almeras and Fournier, 2008).

Equation (16) states that this passive bending is a ratio between (i) the increment in the bending moment, i.e. on the weight increment and on the lever arm related to both the distance to the centre of mass H_G and the local leaning angle γ, and t and (ii) the local flexural stiffness of the organ. It thus depends on the morphology and size of the plant, as well as on the anatomy and size of its cross-section, with a fourth power dependance on the organ radius R (see Almeras and Fournier, 2008, for a more detailed analysis of these resistances, especially the effects of organ size, slenderness, and tapering).

Last but not least, the combination of equations (15) and (16) demonstrates another important growth-mediated constraint on gravitropic movement. If $\Delta\varepsilon_m$ is set to zero (no bending motor), then according to equation (15), no active

change in curvature would occur. However, there is a change in cross-sectional radius R. At the same time, growing weight induces a passive down-bending according to equation (16). If at some point, the regulatory system sets the bending motor on again, then the work to recover from the passive bending will be much higher due to the R inverse-square dependence of the gravitropic motor (equation 15). This is due to the fact that since newly-deposited cell wall layers tend to mould onto existing cell wall, there is a tendency for curvature to become fixed by cell-wall deposition (see Fig. 6 in Moulia *et al.*, 2006) in the absence of motor activity. Thus, growth acts a double constraint on shape, through down-bending and by fixing any curvature, so that without active motor drivers and gravitropic regulation, any axis will tend to droop down and weep (Moulia *et al.*, 2006). This conflict between the motor and fixing consequences of growth is central to the actual shape of many organs (Almeras *et al.*, 2002, 2004; Coutand *et al.*, 2007). It is thus necessary to integrate both motor and resistances with graviperceptive regulation into more complex models in order to get a grasp on the power and control of movements.

Two integrative models of shoot gravitropism

We have seen that the gravitropic response of an organ involves (i) dose-sensitive sensing of the disorientation versus gravity, and possibly other variables too (autotropism), (ii) transduction of this response from the gravisensing cells to the motor cells, (iii) size and anatomy-dependent biomechanical motors, and (iv) internal and external resistances, all of which act non-linearly. Directly handling the combination of all these processes within quantitative arguments is beyond the capacity of the human mind, but formalized models provide suitable tools. Modelling has a long history in gravitropic studies, and some of the equations involved in such models have already been discussed in the previous sections (see Fournier *et al.*, 1994*a*, and Meskauskas *et al.*, 1999*a*, *b*, for reviews). We will focus here on only two models, selected for three reasons: (i) they are among the most recently produced, (ii) they deal with spatial–temporal changes in the curvature field, and (iii) they have been compared with detailed experimentally-derived kinematic data (Meskauskas *et al.*, 1999*a*, *b*; Coutand *et al.*, 2007). Meskauskas' model deals with gravitropism through primary growth, whereas Fournier's model deals with gravitropism through secondary growth. Yet besides their individual interests, comparing the two provides key insights.

Fournier's model was first published in 1994. More complex versions have since been developed (Jirasek *et al.*, 2000; Fourcaud and Lac, 2003; Fourcaud *et al.*, 2003; Almeras *et al.*, 2005; Almeras and Fournier, 2008), but the central elements have remained unchanged. The gravitropic reaction is modelled through the following steps and associated basic equations.

(i) Gravisensing is assumed be locally and uniformly distributed along the stem according to the endodermal starch-sheath theory and the experimental localization of gravisensing (Weize *et al.*, 2000). It displays a dose–response to angle related to equation (7b), but in which the sensed angle is the local angle $\gamma_{(s,t)}$ and not the tip angle. This local graviperception function is held to control the transverse distribution of maturation strain $\Delta\varepsilon_m(s,t)$ through reaction wood differentiation, with negligible lag-time i.e. $\Delta\varepsilon_{m(s,t+dt)} \approx \frac{-k_{SA}\left(\gamma_{(s,t)}-\gamma_{GSA}\right)}{\left|\gamma_{(s,t)}-\gamma_{GSA}\right|}$, with γ_{GSA} and k_{SA} being constants for the species. This equation is a simplification of equation (7b), where only the sign of the angular distortion $\left(\gamma_{(s,t)}-\gamma_{GSA}\right)$ is sensed rather than its exact value.

(ii) The local bending PPS motor is modelled biomechanically taking into account (i) positional effects of tissues laid down by secondary growth within the cross-section, and (ii) the internal resistance of the older core, using equation (15b). The spatio-temporal distribution of secondary growth DR/Dt (s,t) is an input to equation (15b) taken from exogenous data (i.e. assuming no graviperception feedback on the mean rate of secondary growth).

(iii) The resistive bending due to increments of self-weight along the stem and of stem length is modelled using equation (16) and taking into account the detailed shape of the stem. The primary growth dL/dt (where L is total length) and its orientation are taken from exogeneous data.

(iv) The distribution of local inclination angles $\gamma_{(s,t+dt)}$ is then computed from change in curvature $D\kappa/Dt_{(s,t)}$, using spatial integration [equation (2), solved for every position s]. This step requires boundary angular conditions at the base and the tip of the organ. Anchorage is usually assumed to be perfectly stiff (no angular variation of the stem base). The apical primary growing segment is assumed to have achieved its orientation according to γ_{GSA} within one time-step (since primary gravitropism is much faster than secondary gravitropism).

Note that this model only has one parameter (k_{SA}) to be fitted (on an independent dataset); all the other values can be measured directly and independently of the model (although in some studies, some of them were also estimated to avoid overcrowding the measurements). Up to now, growth data (radial and apical growth) are inputs issued from (i) experimental data (Coutand *et al.*, 2007) or (ii) independent growth models (assuming no feedback of graviperception on the mean rates of growth).

This type of model has proved to be able to account for the S-shape of certain branches (Fournier *et al.*, 1994*a*; Jirasek *et al.*, 2000) without the need to assume *ad hoc* variations in GSA γ_{GSA}, as was the case previously (Digby and Firn, 1995). This S-shape is simply due to mechanical competition over time between the downward drooping due to changes in self-weight increasing the lever arm toward the base, and the setting of primary growth direction on the apical zone of the branch and/or the onset of the reaction wood motor and active geotropic reorientation. This explanatory model was assessed experimentally and was found to agree with measured data as long as the Young's modulus was correctly estimated (Almeras *et al.*, 2002). It should be noted that the model was also able to simulate very different

rates of curvature changes $D\kappa/Dt_{(s,t)}$ as a function of position s along the organ, despite a similar graviperceptive function. This is because the local rate of change in curvature depends on stem radius, which usually varies significantly along the stem, especially in woody plants. Indeed, for the motor bending, equation (15) shows that the gravitropic curvature rate scales as $R^{-2}(s,t)$. Thus, even when everything else is kept constant along the stem in equation (15) (stimulation angle, radial growth $dR(s,t)$, cross-section shape, maturation strain, and Young's modulus distribution), the rate of curvature $D\kappa/Dt_{(s,t)}$ is greatly influenced by the taper [i.e. the variations of the radius $R(s)$ along the stem positions). Actually, $D\kappa/Dt_{(s,t)}$ will be significantly lower in the distal thicker parts of the stem. For example, a realistic taper of 1 cm m^{-1} in equation (15) produces a decrease of the curvature rate of $1-\frac{1^2}{2^2}=75\%$ between a 1 cm thick segment and a 2 cm thick one located 1 m below.

In addition, the taper $R(s,t)$ is not usually constant over time during growth. The observed curvature rate $D\kappa/Dt(s,t)$ then comes as the superimposition of the motor bending (equation 15) and the resistive bending due to selfweight growth [equation (16)]. Therefore, the variations along the stem of the curvature rate should be more complex than a simple $R^{-2}(s,t)$ function, although always greatly influenced by taper and size. Without a proper analysis of these effects of size and shape using biomechanical models, there is a high risk of interpreting purely biomechanical consequences of stem geometry on the rate of changes in curvature as biological differences of gravisensing and dose–response functions. This risk is heightened if only the changes in tip angle as a function of its previous inclination angle are monitored (as the tip angle results from the summation of the changes in curvature from $s=0$ to $s=L$—see equation (2)—and is thus dependent on L and on the overall shape of the stem; Fig. 3F). This clearly demonstrates how any attempt to infer differences in gravisensitivity (and/or in GSA) without a good knowledge of the biomechanics of the motor forces and resistances involved can yield very misleading results.

Despite its good predictive behaviour, Fournier's integrative model was recently falsified using a detailed kinematical study of curvature field and growth in poplar trees (Coutand *et al.*, 2007). Some of the discrepancy between the model and the experimental data was due to insufficient knowledge on the kinetics of maturation $\Delta m_{(x,y,s,t)}$. But the major discrepancy was that the model tended to overshoot whereas the real tree never did (see Fig. 5). This discrepancy, which arose mainly from the gravisensing control in the model, clearly pointed towards a more complex control on bending rates than that due to the sine law of gravisensing.

A similar conclusion was reached by Meskauskas and coworkers working with primary organs (Meskauskas and Moore, 1998; Meskauskas *et al.*, 1999*b*) but using more advanced models of graviperception. Consistent with the experimental data on auxin transport, they initially proposed a model combining gravisensing of (i) the tip angle $\gamma_{T(t)}$ according to the sine law equation (7) $S_{T(t)}=\sin(\gamma_{T(t)})$ and (ii) the local angle $\gamma_{(s,t)}$. Several laws for the gravisensing of the local angle have been tested (Meskauskas and Moore, 1998; Meskauskas *et al.*, 1999*a*), and a negative exponential law $S_{L(s,t)}=e^{-k_{SL}\cdot\left(\frac{\Pi}{2}-\gamma_{(s,t)}\right)}$ was the one retained (although no mechanistic grounds in terms of cellular gravisensing could be given up until then). For the two perceptions to act locally at the same s would require a signal transmission from the tip. After testing several transmission laws against experimental data (Meskauskas and Moore, 1998), they ended with a wave transmission at velocity v_T with an exponential decrease in magnitude as it progresses downward $S_{T(s,t)}=S_{T(t-(1-s/L)/v_T)}\cdot e^{-k_T(1-s/L)}$ (Meskauskas *et al.*, 1999*a*). It was assumed that the two signals act additively on the differential growth response, i.e. $\Omega_{(s,t)}=S_{L(s,t)}+S_{T(s,t)}=S_{L(s,t)}+S_{T(t-(1-s/L)/v_T)}\cdot e^{-k_T(1-s/L)}$. No biomechanical modelling of the differential-growth motor was proposed, since, as explained in the previous section, none is yet available. Therefore a direct relationship between the rate of curvature change at position s and the dual gravisensing signal $\Omega(s,t)$ was assumed. As in Fournier's model, the distribution of local inclination angles $\gamma_{(s,t+dt)}$, including the tip angle $\gamma_{T(t)}$, was computed from the change in curvature, using spatial integration [equation (2), solved for every position s]. However, when tested against experimental data, this model turned out to be clearly insufficient (as did all of the other combinations of transmission laws and local perceptive laws; Meskauskas *et al.*, 1999*b*). Three additional ingredients had to be added:

(i) First of all, and principally, an autotropic curvature-compensation mechanism based on curvature sensing (independently of the gravisensing of inclination) has to be included, i.e. $A_{(s,t)}=k_A\cdot\kappa_{(s,t)}$ to make:

$$\Omega(s,t)=S_{L(s,t)}+S_{T(s,t)}+A_{(s,t)} \qquad (17)$$

This is why Meskauskas and coworkers named their model the 'revised local curvature distribution model'.

(ii) Furthermore, a non-uniform capacity for local sensing of both curvature and local angle had to be retained (both were assumed to decrease exponentially from the apex in a basipetal direction).

(ii) Finally, a multiplicative realization coefficient K_w had to be added (probably accounting for the efficiency of the unmodelled motor mechanism in working the active bending).

Using this new set of equations, Meskauskas *et al.* were able to reproduce experimental situations that were not part of the context used to design the model, including responses to different initial angles γ_0 (this was not the case for older models). They were also able to reproduce the fact that gravireacting stems may straighten before overshooting the vertical, and may also reach a steady inclination that is not the vertical without having to introduce an *ad hoc* time-changing GSA. Moreover, this model turned out be relatively generic, able to fit responses of organisms as different as the *Coprinus* stipe and the wheat coleoptile (Meskauskas *et al.*, 1999*a*, *b*). Last but not least, the model could also fit the responses of stems submitted to physiological inhibitors of the gravisensing pathway (i.e. a Ca^{2+} chelator, a Ca^{2+} ionophore, and an inhibitor of the

cytoskeleton formation of F-actin filaments), making it feasible for use as a reverse tool for estimating quantitative physiological effects (Meskauskas *et al.*, 1999*a*).

There are several limitations to the Meskauskas 'revised local curvature distribution model'. One is obviously that it features nine parameters whose estimations can only be achieved using the model. From a statistical perspective of parameter estimation, this is a lot. It becomes necessary to design very large datasets derived from a set of experiments planned to act almost orthogonally on the parameters in the model, so that the estimates of the various parameters are not too correlated. Otherwise, even when the model appears to fit the data well, it could still be due to numerical compensatory artefacts between the parameter values (Tremblay and Wallach, 2004). Despite fitting the model on four cleverly chosen experiments, the current dataset studied by Meskauskas and co-workers does not yet appear sufficiently comprehensive, and there may be a great deal of experimental work to do. That said, if the model could be made less complex, or at least made to use parameters that can be directly measured independently of the model, it would become easier to assess and be extremely useful. The comparison with Fournier's model here may be informative. Meskauskas and co-workers had to model in a decrease in the ability to respond to local sensing of both curvature and local angle, together with a realization coefficient K_w for the curving (i.e. three additional parameters). However, this apparent decrease in curving response along the axis may result from differences in the balance between motor efficiency and mechanical resistance levels all along the organ (as they are known to be diameter and lever-arm-dependent) rather than on *ad hoc* variations in local sensitivities. Including a biomechanical model of both motors and resistances would make it possible to replace these *ad hoc* parameters with biophysical parameters that can be measured directly.

The second limitation of the Meskauskas' model is that it does not, in its present state, take into account the kinematics of expansion growth, as only the local time-derivative $\frac{\partial \kappa_{(s,t)}}{\partial t}$ was considered instead of the material derivative $\frac{D\kappa_{(s,t)}}{Dt}$ [thus neglecting convective changes that were likely to occur due to clear curvature gradients $\frac{\partial \kappa_{(s,t)}}{\partial s}$; see equation (3)]. Some acknowledgement of the effect of expansion growth as introduced by using the relative curvilinear abscissa s/L rather than the absolute value s in the terms of exponential spatial decrease in the three signals, but this is still insufficient, as (i) expansion growth is spatially non-uniform and (ii) the convective effects might be strong.

Despite their limitations (and it is normal for scientific advance that state-of-the-art models are criticized and eventually falsified), taken together, these two models bring a clear convergent perspective.

First of all, the autotropic curvature-compensation mechanism is central to the overall gravitropic-straightening response (Iino, 2006; Moulia *et al.*, 2006). It is not possible to reach the vertical through bending, and so counter-bending is necessary in order to get straight. Moreover, autotropic curvature sensing acts concomitantly with gravisensing, and both drive the bending motor. As soon as gravitropic curvature starts, autotropic curvature compensation is activated. Therefore, only the very initial rate of curvature changes may actually be measuring the response to gravisensing, but to be measured accurately requires highly sensitive spatio-temporal kinematical measurements, such as the recent bio-imaging methods. Estimates of angles such as the one shown in Fig. 2A are clearly a measure of the steady balance between gravitropic and autotropic sensing (Meskauskas *et al.*, 1999*b*), and do not serve to characterize gravisensitivity.

Second, it is not possible to analyse gravisensitivity and its possible changes during the graviresponse without considering (i) the distribution of the curvature response (and of the growth response), and (ii) without having a good estimation of the powers of the motor and of the various resistances, as these depend biomechanically on cross-sectional size and anatomy, as well as on organ length and specific weight. Only then does it become possible to tackle the important issues of varying sensitivity and possible accommodation (Moulia *et al.*, 2006) of the gravi- and mechano-sensing system. A good example of a model providing direct access to local gravisensitivity is the work by Yamashita *et al.* (2007) in tree stems. As shown previously, the gravitropic response is mediated by reaction wood formation according to the PPS motor and Fournier's model [equations (15) and (16)], and the variable controlled by gravisensing is maturation strain $\Delta\varepsilon_m$. Yamashita *et al.* (2007) maintained the stem attached to a stiff stake. This confers three advantages. The most obvious is that the stimulation angle γ is maintained constant and the presentation time t_s can be controlled. But there is more. Using the biomechanical model of the motor and the resistance to bending, it can be shown that restraining any bending results in an override of the resisting effects of the inner core and the self-weight, so that a very accurate estimation of the $\Delta\varepsilon_m$ input to the PPS motor can be measured directly. An accurate local dose–response curve could thereby be determined for the gravitropic motor input. The authors found that maturation strains increased for stimulation angles γ smaller than 30° and then saturated, a function differing from a sine law and radically different from a negative exponential.

Third, formalized models integrating physiological and mechanical processes are highly useful tools for handling and analysing the complexity of organ response. Gravitropism is a feedback process where current geometrical configuration is sensed and influences the next step. Too much focus on the so-called initial phases is likely to hinder some very significant mechanisms (even the gravisensing mechanism itself). This might be highly detrimental when analysing physiological responses such as that of inhibitors, or when phenotyping mutants. Consider the case of mutants or inhibitors affecting cytoskeleton dynamics (Palmieri *et al.*, 2007). Cytoskeleton dynamics is known potentially to affect statolith movements (Morita and Tasaka, 2004), mechanosensing (Perbal and Driss-Ecole, 2003), PIN relocalization, cell wall growth (Ikushima *et al.*, 2008), and the list could well go on! Using integrative

models and related experiments, it might be possible quantitatively to analyse the individual contributions of these effects to the overall gravitropic phenotype (Meskauskas *et al.*, 1999*b*; Moulia *et al.*, 2006).

To round up, integrative models can be used to analyse the effect of genetic variation in the parameter values (due to natural quantitative variations, mutations, or genetic engineering) for phenotypic performance (Tardieu, 2003). This leads us to our last point, namely the ecological significance of gravitropism.

Back to the HMS Beagle: natural diversity in shoot gravitropism and its adaptive significance

It is usually considered that a major motivation for Charles Darwin in his studies following '*On the origin of species*' was to study the natural variation of traits in living beings and to gain further insights into possible natural selection. Indeed, '*The power of movement in plants'*, studied many different species. It is, however, striking that, until only recently, very little consideration had been given to the ecological significance of variations in gravitropism response. This is probably because focus was given solely to the obvious role of gravitropism in seedlings. In '*The power of movement in plants*', the ecological function of gravitropism is dealt with in the Introduction, stating basically that gravitropisms make it possible for the seedling shoot to find its way up, even if it is buried in the soil, and for the radicle to find its way down into the soil. More efficiency in this process might affect germination success, but this is only one of the many environmental selective pressures acting on seedling survival (Coomes and Grubb, 2003). Although often noted in passing, the life-long central importance of gravitropism and autotropism in land-growing plants has only recently been stressed (Mosbrugger, 1990; Iino *et al.*, 2006; Moulia *et al.*, 2006; Almeras and Fournier, 2008). Indeed, gravi-autotropism provides the plant with (i) the ability to regulate posture and (ii) the ability actively to recover from non-lethal mechanical hazards such as moderate windthrow, soil slipping, or mechanical buckling under self-weight (Moulia *et al.*, 2006). Different species or different plant stages might involve different motors, but all land-erected plants have the power of movement through an active motor (actually, in most plants, several motors can act simultaneously; Hay *et al.*, 2000; Moulia *et al.*, 2006). Moreover, it has been proposed that the adaptive significance of gravi-auto-tropisms is linked to the mechanical dimensioning of the plant body through thigmomorphogenesis (Moulia *et al.*, 2006) and photomorphogenesis (Fournier *et al.*, 2006). Thigmomorphogenesis is the central process in adapting the plant's mechanical structure to fit its mechanical environment (wind, slope, self-weight, etc.). Gravi-autotropic recovery plays a particularly important role when plants have to undertake risks, either by growing tall and thin under dim light to reach the canopy (Fournier *et al.*, 2006; Iino, 2006) or by suddenly having to cope with much more wind drag when overtopping other plants (de Langre, 2008).

It has been shown that there is considerable interpecific variability in the performances of the gravisensing systems. Variations of one order of magnitude in the apparent presentation time τ_p between species have been reported (Audus, 1969), ranging from less than a minute up to several hours. More recently, ecotypic variations have also been described. Considering the inflorescence stems of *Arabidopsis* grown under the same controlled conditions, Tanimoto *et al.* (2008) reported that most of the amyloplasts reached the apical side of statocytes within 20 min in the Col ecotype compared to 60 min in L*er*, which equates to a factor of 3 in presentation times. Sierra *et al.* (2008) demonstrated that ecotypes of pine (*Pinus pinaster* Ait) displayed very large differences in gravitropic efficiency (due to differences in the response of the differential maturation strain to inclination angle) as well as in their autotropic capacity. High gravitropic motor and autotropic control efficiencies yielded much improved adult trunk straightness in provenance trials, giving rise to interesting selection criteria for plant breeding (and maybe for natural selection?). Note, incidentally, that this analysis in Sierra *et al.* (2008) was achieved using integrative biomechanical models.

Lastly, Fournier *et al.* (2006), studying the communities with the highest biodiversity on Earth, the rain forests, demonstrated through extensive surveys on a community of tree species that 92% of sapling stems display active gravitropic movement either compensating (9%) or overtopping (81%) growth-induced downward-drooping, highlighting the prevalence of gravitropic control. Since there are still no available long-term kinematical studies on trees (which, by definition, would have to run over decades), this analysis employed integrative biomechanical models. Moreover, the very large interspecific variation in *in situ* gravitropic performance and in gravitropic capacity in optimally-controlled environments could be correlated with the amount of mechanical risk the species faces in its environment. This clearly raises the possibility of integrated biomechanical strategies for height growth in land plants (Fournier *et al.*, 2006; Moulia *et al.* 2006). The significance of this in terms of functional land ecosystem ecology and evolutionary biology (Mosbrugger, 1990) has yet to be studied, but there is no doubt that integrative biomechanical models will provide pivotal input by helping define relevant 'hard' process-based traits and estimating them in large populations (Fournier *et al.*, 2006; Sierra *et al.*, 2008). However, this would also require a more concerted ecological research effort covering various situations, but can be expected to bring many insights (Fournier *et al.*, 2006; Iino, 2006), just as HMS Beagle's journey was instrumental to Charles Darwin's work.

Conclusion

Over almost 130 years, huge advances have been made in our understanding of gravitropic movement in plants. We

have gained a great deal of insight into the underlying molecular mechanisms, and biomechanical studies together with spatial microgravity studies have revealed the role played by physics in the process. Nevertheless, in the context of this review, it is striking to see how far the current explanatory models and tools can be traced back to Darwins' time: examples include the starch-statolith hypothesis, osmo-hydraulic motors, and growth kinematics, to name but a few.

To some extent, though, the last few decades have been characterized by discipline segmentation and increasingly specialized studies. This has clearly been rewarding, as the process has produced efficient tools and numerous facts that have pushed back the boundaries of plant physiology. However, limits to this segmentation may now have been reached. There are clear needs and rewards for interdisciplinary approaches involving modern physics and biology in the field of gravitropism; some of the insights already brought by such approaches have been presented in this review. Mathematical modelling coupled with high-resolution bio-imaging are proving to be powerful tools, and can be expected to drive gravitropic studies into the realm of modern systems biology.

Modelling has turned out to be a more accurate way of setting and testing hypotheses dealing with the non-linear dynamic systems involved in gravitropism, as long as these models are assessed continuously with crucial experiments. Integrative models are also likely to be extremely helpful in evaluating and rating the efficiency of the control of a given gene on the overall performance of the shoot. They also therefore lend themselves perfectly to phenotyping plant gravitropic mutants, and to defining relevant gravitropic traits for ecological study.

Our review on the state-of-the-art in gravitropic modelling has revealed at least four domains where the development of integrative biomechanical modelling would offer rewards: (i) integrative models of cellular gravisensing, including statoliths and their collective dynamics as well as their interactions with molecular motors and vesicular trafficking; (ii) integrative models of the primary bending motor, and of its genetic controls; (iii) models of the interplay between gravitropism and autotropism (and phototropism) in the control of gravitropic movement and the signalling required for it to be co-ordinated in a given organ as well as across the entire plant architecture (Trewavas, 2003; Moulia *et al.*, 2006; Fourcaud *et al.*, 2008), and (iv) population and community models in ecology, analysing the significance of genetic variation in gravitropism and, more generally, the significance of biomechanical height growth strategies in ecosystem function and, ultimately, for the fitness of plant species in different environments. This more integrated and interdisciplinary view might take us deeper into the research agenda on the power of movement in plants and its ecological significance, an agenda originally drawn 150 years ago.

Acknowledgements

We thank Dr C Girousse and R Bastien for reading the ms, Mr McCulley from A-T-T (http://www.a-t-t.fr), for carefully proof-reading the ms for the English, and an anonymous reviewer for useful suggestions. This work has been supported by ANR-05-BDIV-012-03 'Woodiversity'.

References

Almeras T, Costes E, Salles JC. 2004. Identification of biomechanical factors involved in stem shape variability between apricot tree varieties. *Annals of Botany* **93,** 455–468.

Almeras T, Fournier M. 2008. Biomechanical design and long-term stability of trees: morphological and wood traits involved in the balance between weight increase and the gravitropic reaction. *Journal of Theoretical Biology* (in press).

Almeras T, Gril J, Costes E. 2002. Bending of apricot tree branches under the weight of axillary growth: test of a mechanical model with experimental data. *Trees* **16,** 5–15.

Almeras T, Thibaut A, Gril J. 2005. Effect of circumferential heterogeneity of wood maturation strain, modulus of elasticity and radial growth on the regulation of stem orientation in trees. *Trees* **19,** 457–467.

Almeras T, Yoshida M, Okuyama T. 2006. Generation of longitudinal maturation stress is not related to diurnal changes in diameter. *Journal of Wood Science* **52,** 452–455.

Archer RR. 1987. *Growth stresses and strains in trees*. Berlin: Springer.

Audus LJ. 1964. Geotropism and the modified sine rule; an interpretation based on the amyloplast statolith theory. *Physiologia Plantarum* **17,** 737–745.

Audus LJ. 1969. Geotropism. In: Wilkins MB, ed. *The physiology of plant growth and development*. London: McGraw-Hill, 203–241.

Basu P, Pal A, Lynch JP, Brown KM. 2007. A novel image-analysis technique for kinematic study of growth and curvature. *Plant Physiology* **145,** 305–316.

Ben Amar M, Goriely A. 2005. Growth and instability in elastic tissues. *Journal of the Mechanics and Physics of Solids* **53,** 2284–2319.

Bennett MJ, Roberts J, Palme K. 2000. Moving on up: auxin-induced K^+ channel expression regulates gravitropism. *Trends in Plant Science* **5,** 85–86.

Blancaflort EB, Masson PH. 2003. Plant gravitropism. Unraveling the ups and downs of a complex process. *Plant Physiology* **133,** 1677–1690.

Boyer JS, Silk WK. 2004. Hydraulics of plant growth. *Functional Plant Biology* **31,** 761–773.

Burgert I, Eder M, Gierlinger N, Fratzl P. 2007. Tensile and compressive stresses in tracheids are induced by swelling based on geometrical constraints of the wood cell. *Planta* **226,** 981–987.

Chavarria-Krauser A. 2006. Quantification of curvature production in cylindrical organs, such as roots and hypocotyls. *New Phytologist* **171,** 633–641.

Chavarria-Krauser A, Nagel KA, Palme K, Schurr U, Walters A, Scarr H. 2008. Spatio-temporal quantification of differential processes in root growth zones based on a novel combination of image sequence processing and refined concepts describing curvature production. *New Phytologist* **177,** 811–821.

Clair B, Almeras T, Sugiyama J. 2006. Compression stress in opposite wood of angiosperms: observations in chestnut, mani and poplar. *Annals of Forest Science* **63,** 507–510.

Clair B, Alméras T, Yamamoto H, Okuyama T, Sugiyama J. 2007. Mechanical behavior of cellulose microfibrils in tension wood, in relation with maturation stress generation. *Biophysical Journal* **91,** 1128–1135.

Coen E, Rolland-Lagan AG, Matthews M, Bangham JA, Prusinkiewicz P. 2004. The genetics of geometry. *Proceedings of the National Academy of Sciences, USA* **101,** 4728–4735.

Coomes DA, Grubb PJ. 2003. Colonization, tolerance, competition and seed-size variation within functional groups. *Trends in Ecology and Evolution* **18,** 283–291.

Correll MJ, Kiss JZ. 2008. Space-based research on plant tropisms. In: Gilroy S, Masson PH, eds. *Plant tropisms*. Oxford, UK: Blackwell Publishing, 161–182.

Cosgrove DJ. 1990*a*. Rapid, bilateral changes in growth rate and curvature during gravitropism of cucumber hypocotyls: implications for mechanisms of growth control. *Plant*, *Cell and Environment* **13,** 227–234.

Cosgrove DJ. 1990*b*. Gravitropism of cucumber hypocotyls: biophysical mechanism of altered growth. *Plant, Cell and Environment* **13,** 235–241.

Coutand C, Fournier M, Moulia B. 2007. Gravitropic response of polar trunk: key roles of the regulation of wood prestressing and of relative kinetics of cambial growth versus wood maturation. *Plant Physiology* **144,** 1166–1180.

Coutand C, Moulia B. 2000. Biomechanical study of the effect of a controlled bending on tomato stem elongation. II. Local strain sensing and spatial integration of the signal. *Journal of Experimental Botany* **51,** 1825–1842.

Darwin C, Darwin F. 1880. *The power of movements in plants*. London, England: Murray.

de Langre E. 2008. Effects of wind on plants. *Annual Review of Fluid Mechanics* **40,** 141–168.

Digby J, Firn RD. 1995. The gravitropic set-point angle (GSA): the identification of an important developmentally controlled variable governing plant architecture. *Plant, Cell and Environment* **18,** 1434–1440.

Dolk H. 1936. Geotropism and the growth substance. *Recueil des Travaux Botaniques Néerlandais* **33,** 509–585.

Du S, Yamamoto F. 2007. An overview of the biology of reaction wood formation. *Journal of Integrative Plant Biology* **49,** 131–143.

Dumais J, Shaw SL, Steele CR, Long SR, Ray PM. 2006. An anisotropic-viscoplastic model of plant cell morphogenesis by tip growth. *International Journal of Developmental Biology* **50,** 209–222.

Edwards CH, Penney DE. 1994. *Calculus with analytical geometry*. New Jersey, USA: Prentice Hall, Englewoods Cliffs.

Firn RD, Digby J. 1979. A study of autotropic straightening reaction of a shoot previously curved during geotropism. *Plant, Cell and Environment* **2,** 149–154.

Firn RD, Digby J. 1980. The establishment of tropic curvatures in plants. *Annual Review of Plant Physiology* **31,** 131–148.

Firn RD, Digby J, Hall LA. 1981. The role of the shoot apex in geotropism. *Plant, Cell and Environment* **4,** 125–129.

Fourcaud T, Blaise F, Lac P, Castera P, Reffye Pd. 2003. Numerical modelling of shape regulation and growth stresses in trees. II. Implementation in the AMAPpara software and simulation of tree growth. *Trees: Structure and Function* **17,** 31–39.

Fourcaud T, Lac P. 2003. Numerical modelling of shape regulation and growth stresses in trees. I. An incremental static finite element formulation. *Trees: Structure and Function* **17,** 23–30.

Fourcaud T, Zhang X, Stokes A, Lambers H, Korner C. 2008. Plant growth modelling and applications: the increasing importance of plant architecture in growth models. *Annals of Botany* **101,** 1053–1063.

Fournier M, Baillères H, Chanson B. 1994*a*. Tree biomechanics: growth, cumulative prestresses and re-orientations. *Biomimetics* **2,** 229–251.

Fournier M, Chanson B, Thibaut B, Guitard D. 1994*b*. Measurements of residual growth strains at the stem surface: observations on different species. *Annals of Forest Science* **51,** 249–266 (in French).

Fournier M, Stokes A, Coutand C, Fourcaud T, Moulia B. 2006. Tree biomechanics and growth strategies in the context of forest functional ecology. In: Herrel A, Speck T, Rowe N, eds. *Ecology and biomechanics: a biomechanical approach of the ecology of animals and plants*. Boca Raton, Florida, USA: CRC Taylor and Francis, 1–33.

Fukaki H, Fujisawa H, Tasaka M. 1996. Gravitropic response of inflorescence stems in *Arabidopsis thaliana*. *Plant Physiology* **110,** 933–943.

Galland P. 2002. Tropisms of *Avena* coleoptiles: sine law for gravitropism, exponential law for photogravitropic equilibrium. *Planta* **215,** 779–784.

Gilroy S, Masson PH. 2008. *Plant tropisms*. Oxford, UK: Blackwell Publishing.

Girousse C, Moulia B, Silk W, Bonnemain JL. 2005. Aphid infestation causes different changes in carbon and nitrogen allocation in alfalfa stems as well as different inhibitions of longitudinal and radial expansion. *Plant Physiology* **137,** 1474–1484.

Haga K, Iino M. 2006. Asymmetric distribution of auxin correlates with gravitropism and phototropism but not with autostraightening (autotropism) in pea epicotyls. *Journal of Experimental Botany* **57,** 837–847.

Harisson BR, Morita MT, Masson PH, Tasaka M. 2008. Signal transduction in gravitropism. In: Gilroy S, Masson PH, eds. *Plant tropisms*. Oxford, UK: Blackwell Publishing, 21–46.

Haswell ES. 2003. Gravity perception: how plants stand up for themselves. *Current Biology* **13,** R761–R763.

Hay J, Moulia B, Silk WK, Lane B, Freeling M. 2000. Biomechanical analysis of the rolled (Rld) leaf phenotype of maize. *American Journal of Botany* **87,** 625–633.

Hejnowicz Z. 1997. Graviresponses in herbs and trees: a major role for the redistribution of tissue and growth stresses. *Planta* **203,** S136–S146.

Hoshino T, Miyamoto K, Ueda J. 2007. Gravity-controlled asymmetrical transport of auxin regulates a gravitropic response in the early growth stage of etiolated pea (*Pisum sativum*) epicotyls: studies using simulated microgravity conditions on a three-dimensional clinostat and using an agravitropic mutant, *ageotropum*. *Journal of Plant Research* **120,** 619–628.

Hughes-Hallet D, Gleason AM, Frazer Lock P, Flath DE, Gordon SP, Lomen DO, Lovelock D, McCallum WG, Osgood BG, Pasquale A. 1996. *Applied calculus: for business, social sciences and life sciences*. NY, USA: John Wiley & Sons.

Iino M. 2006. Toward understanding the ecological functions of tropisms: interactions among and effects of light on tropisms. *Current Opinion in Plant Biology* **9,** 89–93.

Iino M, Tarui Y, Uematsu C. 1996. Gravitropism of maize and rice coleoptiles: dependence on the stimulation angle. *Plant, Cell and Environment* **19,** 1160–1168.

Ikushima T, Shimmen T. 2005. Mechano-sensitive orientation of cortical micrtotubules during gravitropism in azuki bean epicotyls. *Journal of Plant Research* **118,** 19–26.

Ikushima T, Soga K, Hoson T, Shimmen T. 2008. Role of xyloglucan in gravitropic bending of azuki bean epicotyl. *Physiologia Plantarum* **132,** 552–565.

Jirasek C, Prusinkiewicz P, Moulia B. 2000. Integrating biomechanics into developmental plant models expressed using Lsystems. In: Spatz H-C, Speck T, eds. *Plant biomechanics, 2000*. Third Plant Biomechanics Conference. Freiburg, Germany: Thieme Verlag, Stuttgart, Germany, 615–624.

Johansen JN, Vernhettes S, Hofte H. 2006. The ins and outs of plant cell walls. *Current Opinion in Plant Biology* **9,** 616–620.

Kiss JZ. 2000. Mechanisms of the early phases of plant gravitropism. *Critical Reviews in Plant Sciences* **19,** 551–573.

Krupkova E, Immerzeel P, Pauly M. 2007. The *TUMOROUS SHOOT DEVELOPMENT2* gene of *Arabidopsis* encoding a putative methyltransferase is required for cell adhesion and co-ordinated plant development. *The Plant Journal* **50,** 735–750.

Kutschera U. 2001. Gravitropism of axial organs in multicellular plants. *Advances in Space Research* **27,** 851–860.

Kutschera U. 2008. The pacemaker of plant growth. *Trends in Plant Science* **13,** 105–107.

Kutschera U, Niklas KJ. 2007. The epidermal-growth-control theory of stem elongation: an old and a new perspective. *Journal of Plant Physiology* **164,** 1395–1409.

LaMotte CE, Pickard BG. 2004. Control of gravitropic orientation. I. Non-vertical orientation by primary roots of maize results from decay of competence for orthogravitropic induction. *Functional Plant Biology* **31,** 93–107.

Larsen P. 1969. The optimum angle of geotropic stimulation and its relation to the starch statolith hypothesis. *Physiologia Plantarum* **22,** 469–488.

Lockhart JA. 1965. An analysis of irreversible plant cell elongation. *Journal of Theoretical Biology* **8,** 264–275.

Mellerowicz EJ, Sundberg B. 2008. Wood cell walls: biosynthesis, developmental dynamics and their implications for wood properties. *Current Opinion in Plant Biology* **11,** 293–300.

Meskauskas A, Moore D. 1998. Mathematical modelling of morphogenesis in fungi. 1. Spatial organization of the gravitropic response in the mushroom stem of *Coprinus cinereus*. *New Phytologist* **143,** 387–399.

Meskauskas A, Jurkoniene S, Moore D. 1999*a*. Spatial organization of the gravitropic response in plants: applicability of the revised local curvature distribution model to *Triticum aestivum* coleoptiles. *New Phytologist* **140,** 111–123.

Meskauskas A, Moore D, Novak Frazier LA. 1999*b*. Mathematical modelling of morphogenesis in fungi. 2. A key role for curvature compensation ('autotropism') in the local curvature distribution model. *New Phytologist* **143,** 387–399.

Miyamoto K, Katsuhara M, Ookawa T, Kasamo K, Hirasawa T. 2005. Hydraulic conductivity and aquaporins of cortical cells in gravitropically bending roots of *Pisum sativum* L. *Plant Production Science* **8,** 515–524.

Morita MT, Tasaka M. 2004. Gravity sensing and signalling. *Current Opinion in Plant Biology* **7,** 712–718.

Mosbrugger V. 1990. The tree habit in land plants. A functional comparison of trunk constructions with a brief introduction into the biomechanics of trees. In: Bhattacharji SF, Gerald M, Neugebauer HJ, Seilacher A, eds. *Lecture notes in earth sciences,* Vol. 28. Berlin, Heidelberg: Springer-Verlag, 158.

Moulia B. 2000. Leaves as shell structures: double curvature, autostresses and minimal mechanical energy constraints on leaf rolling in grasses. *Journal of Plant Growth Regulation* **19,** 19–30.

Moulia B, Coutand C, Lenne C. 2006. Posture control and skeletal mechanical acclimation in terrestrial plants: implications for mechanical modeling of plant architecture. *American Journal of Botany* **93,** 1477–1489.

Moulia B, Fournier M. 1997. Mechanics of the maize leaf: a composite beam model of the midrib. *Journal of Materials Science* **32,** 2771–2780.

Moulia B, Fournier M, Guitard D. 1994. Mechanics and form of the maize leaf: *in vivo* qualification of the flexural behaviour. *Journal of Materials Science* **29,** 2359–2366.

Muday GK, Rahman A. 2008. Auxin transport and the integration of gravitropic growth. In: Gilroy S, Masson PH, eds. *Plant tropisms*. Oxford, UK: Blackwell Publishing, 47–78.

Mullen JL, Ishikawa H, Evans ML. 1998. Analysis of changes in relative elemental growth rate patterns in the elongation zone of *Arabidopsis* roots upon gravistimulation. *Planta* **206,** 598–603.

Myers AB, Glyn GH, Digby J, Firn RD. 1995. The effect of displacement angle on the gravitropic and autotropic growth responses of sunflower hypocotyls. *Annals of Botany* **75,** 277–280.

Nakamura M, Negishi Y, Funada R, Yamada M. 2001. Sedimentable amyloplasts in starch sheath cells of woody stems of japanese cherry. *Advances in Space Research* **27,** 957–960.

Ortega JKE. 1994. Plant and fungal cell growth: governing equations for cell wall extension and water transport. *Biomimetics* **2,** 215–228.

Palmieri M, Schwind MA, Stevens MHH, Edelmann RE, Kiss JZ. 2007. Effects of the myosin ATPase inhibitor 2,3-butanedione monoxime on amyloplast kinetics and gravitropism of *Arabidopsis* hypocotyls. *Physiologia Plantarum* **130,** 613–626.

Passioura JB, Boyer JS. 2003. Tissue stresses and resistance to water flow conspire to uncouple the water potential of the epidermis from that of the xylem in elongating plant stems. *Functional Plant Biology* **30,** 325–334.

Patten AM, Jourdes M, Brown EE, Laborie MP, Davin LB, Lewis NG. 2007. Reaction tissue formation and stem tensile modulus properties in wild-type and *p*-coumarate-3-hydroxylase downregulated lines of alfalfa. *Medicago sativa (Fabaceae). American Journal of Botany* **94,** 912–925.

Perbal G, Driss-Ecole D. 2003. Mechanotransduction in gravisensing cells. *Trends in Plant Science* **8,** 498–504.

Perbal G, Jeune B, Lefranc A, Carnero-Diaz E, Driss-Ecole D. 2002. The dose–response curve of the gravitropic reaction: a re-analysis. *Physiologia Plantarum* **114,** 336–342.

Peters WS, Tomos AD. 1996. The history of tissue tension. *Annals of Botany* **77,** 657–665.

Peters WS, Tomos AD. 2000. The mechanical state of 'inner tissues' in the growing zone of sunflower hypocotyls and the regulation of its growth rate following excision. *Plant Physiology* **123,** 605–612.

Pfeffer WFP. 2008. Encyclopædia Britannica. *Encyclopædia Britannica 2007 Ultimate Reference Suite*. Chicago: Encyclopædia Britannica.

Philippar K, Fuchs I, Luthen H, *et al*. 1999. Auxin-induced K^+ channel expression represents an essential step in coleoptile growth and gravitropism. *Proceedings of the National Academy of Sciences, USA* **96,** 12186–12191.

Pickard BG. 1973. Geotropic response of the *Avena* coleoptile. 1. Dependence on angle and duration of stimulation. *Canadian Journal of Botany* **51,** 1003–1021.

Power. 2008. Encyclopædia Britannica. *Encyclopædia Britannica 2007 Ultimate Reference Suite*. Chicago: Encyclopædia Britannica.

Sachs JV. 1882. Vorlesungen über Pflanzenphysiologie (Lectures on the Physiology of Plants). New York, USA: Oxford.

Saito C, Morita MT, Kato T, Tasaka M. 2005. Amyloplasts and vacuolar membrane dynamics in the living graviperceptive cell of *Arabidopsis* inflorescence stem. *The Plant Cell* **17,** 548–558.

Salisbury FB, Ross CW. 1992. The power of movement. In: Salisbury FB, Ross CW, eds. *Plant physiology*. Belmont, California, USA: Wadsworth, 408–437.

Schleckler S. 2002. Asymmetric cambial growth and reaction wood of the Late Devonian progymnosperm *Archaeopteris*. *Botany 2002*. Annual Scientific Conference: Madison, Wisconsin, 51–57.

Schmundt D, Stitt M, Jähne B, Schurr U. 1998. Quantitative analysis of local growth rates of dicot leaves at high temporal and spatial resolution, using sequence analysis. *The Plant Journal* **16,** 505–514.

Selker ML, Sievers A. 1987. Analysis of extension and curvature during the graviresponse in *Lepidium* roots. *American Journal of Botany* **74,** 1863–1871.

Sharon E, Roman B, Marder M, Shin GS, Swinney HL. 2002. Mechanics: buckling cascades in free sheets: waxy leaves may not depend only on their genes to make their edges crinkle. *Nature* **419,** 579.

Sierra de Grado R, Pando V, Martinez-Zurimendi P, Penalvo A, Bascones E, Moulia B. 2008. Biomechanical differences in the stem straightening process among *Pinus pinaster* provenances. A new approach for early selection of stem straightness. *Tree Physiology* **28,** 835–846.

Silk W. 1984. Quantitative descriptions of development. *Annual Review of Plant Physiology* **35,** 479–518.

Silk W, Erickson RO. 1978. Kinematics of hypocotyl curvature. *American Journal of Botany* **65,** 310–319.

Stankovic B, Volkmann D. 1998. Autotropism, automorphogenesis and gravity. *Physiologia Plantarum* **102,** 328–335.

Suppato W, Debarre D, Moulia B, Brouzès B, Martin JL, Farge E, Beaurepaire E. 2005. *In vivo* modulation of morphogenetic movements in *Drosophila* embryos with femtosecond laser pulses. *Proceedings of the National Academy of Sciences, USA* **102,** 1047–1052.

Tanaka H, Dhonukshe P, Brewer PB, Friml J. 2006. Spatiotemporal asymmetric auxin distribution: a means to coordinate plant development. *Cellular and Molecular Life Science* **63,** 2738–2754.

Tanimoto M, Tremblay R, Colasanti J. 2008. Altered gravitropic response, amyloplast sedimentation and circumnutation in the *Arabidopsis* shoot gravitropism 5 mutant are associated with reduced starch levels. *Plant Molecular Biology* **67,** 57–69.

Tardieu F. 2003. Virtual plants: modelling as a tool for the genomics of tolerance to water deficit. *Trends in Plant Science* **8,** 9–14.

Tarui Y, Iino M. 1997. Gravitropism of oat and wheat coleoptiles: dependence on the stimulation angle and the involvement of autotropic straightening. *Plant Cell Physiology* **38,** 1346–1353.

Tasaka M, Kato T, Fukaki H. 1999. The endodermis and shoot gravitropism. *Trends in Plant Science* **4,** 103–107.

Telewski F. 2006. A unified hypothesis of mechanoperception in plants. *American Journal of Botany* **93,** 1466–1476.

Tomos AD, Malone M, Pritchard J. 1989. The biophysics of differential growth. *Environmental and Experimental Botany* **29,** 7–23.

Tremblay M, Wallach D. 2004. Comparison of parameter estimation methods for crop models. *Agronomie* **24,** 351–365.

Trewavas A. 2003. Aspects of plant intelligence. *Annals of Botany* **92,** 1–20.

Valster AH, Blancaflort EB. 2008. Mechanisms of gravity perception in higher plants. In: Gilroy S, Masson PH, eds. *Plant tropisms*. Oxford, UK: Blackwell Publishing, 3–20.

van der Weele CM, Jiang HS, Palaniappan KK, Ivanov VB, Palaniappan K, Baskin TI. 2003. A new algorithm for computational image analysis of deformable motion at high spatial and temporal resolution applied to root growth. Roughly uniform elongation in the meristem and also, after an abrupt acceleration, in the elongation zone. *Plant Physiology* **132,** 1138–1148.

Weise SE, Kuznetsov OA, Hasenstein KH, Kiss JZ. 2000. Curvature in Arabidopsis inflorescence stems is limited to the region of amyloplast displacement. *Plant and Cell Physiology* **41,** 702–709.

Wolverton C, Ishikawa H, Evans ML. 2002. The kinetics of root gravitropism: dual motors and sensors. *Journal of Plant Growth Regulation* **21,** 102–112.

Yamashita S, Yoshida M, Takayama S, Okuyama T. 2007. Stem-righting mechanism in Gymnosperm trees deduced from limitations in compression wood development. *Annals of Botany* **99,** 487–493.

Yoshida M, Okuyama T. 2002. Techniques for measuring growth stress on the xylem surface using strain and dial gauges. *Holzforschung* **56,** 461–467.

Yoshihara T, Iino M. 2007. Identification of the gravitropism-related rice gene LAZY1 and elucidation of LAZY1-dependent and -independent gravity signaling pathways. *Plant and Cell Physiology* **48,** 678–688.